Isotope hydrology (^{2}H and ^{18}O) of Ikka fjord and its tufa columns, SW Greenland

BJØRN BUCHARDT, GABRIELLE STOCKMANN, MARC O. HANSEN & ÁRNY SVEINBJÖRNSDÓTTIR

From 1995 to 2022, several expeditions have visited the small Ikka fjord in SW Greenland to study growth and stability of the more than 1000 submarine tufa columns build of the metastable, cold-water carbonate *ikaite* ($CaCO_3 \cdot 6H_2O$). The different water types in the area have been sampled for geochemical and stable isotope (^{2}H and ^{18}O) investigations. Here we present the results of more than 300 isotope analyses of water from the fjord and from streams, lakes, springs and tufa columns. Fjord water samples identify a two-component mixing system ($R^2 > 0.99$) between freshwater runoff and sea water entering from the Davis Strait. The freshwater samples have an average composition of –95.4‰ δ^2H and –13.1‰ δ^{18}O. We find both seasonal and altitude effects in fresh water related to early (June–July) or late (August) sampling time. All freshwater samples excluding lakes but including previous precipitation data (GNIP, 1963–1974) can be described by a Local Meteoric Water Line with slope of 6.43 ± 0.12 and offsets between 6.34 and 6.56. Column water samples are mixed with fjord water but extrapolation to a chlorine-free composition defines an endmember composition of –102‰ δ^2H and –14.2‰ δ^{18}O. These compositions identify precipitation on top of the igneous plateau at ~ 500 m altitude as the source for the column water.

Bjørn Buchardt [bjorn.buchardt@mail.dk], Overgaden neden Vandet 5A,1.tv., DK-1414, Copenhagen K, Denmark. Gabrielle Stockmann [gabrielle@hi.is], Jarvik Geoconsulting AB, Gothenburg, Sweden and Department of Earth Sciences, University of Iceland, Reykjavik, Iceland. Marc O. Hansen [marcowater@yahoo.com], Danish Nature Agency, DK-4500, Nykøbing Sjælland, Denmark. Árný Sveinbjörnsdóttir [arny@hi.is], Institute of Earth Sciences, University of Iceland, Reykjavik, Iceland.

The small Ikka fjord in Arctic south-west Greenland (Fig. 1) has been the focus of several multidisciplinary expeditions between 1995 and 2022. The major purpose was to investigate the occurrence and formation of the more than one thousand submarine tufa columns (named *Ikka Columns*, Fig. 2) in the inner part of the fjord (Pauly 1963a; Buchardt *et al.* 1997, 2001; Hansen *et al.* 2011; Seaman & Buchardt 2006; Seaman *et al.* 2022; Stockmann *et al.* 2022). As part of these activities, many additional studies were carried out including zoological, botanical, microbiological, geochemical and geophysical investigations. A hydrological sampling program in and around the fjord collected more than 375 water samples over three decades for geochemical and stable isotope (^{2}H/^{1}H and ^{18}O/^{16}O) analyses (Table 1). Of this large data base, only a few stable isotope results have been published so far (Buchardt *et al.* 2001).

Stable isotope ratios of water (^{2}H/^{1}H and ^{18}O/^{16}O expressed as δ-functions) are valuable tracers of hydrological systems as they are a property of the water molecule itself. Since the pioneering work by Dansgaard (1964), numerous studies have dealt with the stable isotope composition of all types of water from all parts of the Earth. The relationship between δ^2H and δ^{18}O in meteoric waters is well established and is expressed by the Global Meteoric Water Line (GMWL) equation (Craig 1961; modified by Rozanski *et al.* 1993):

$$\delta^2H = 8.17 \times \delta^{18}O + 10.35, \quad R^2 = 0.98, \quad n = 205$$

Several studies have demonstrated how this relationship is valid only for general use, whereas local conditions may lead to different correlations as expressed by the so-called Local Meteoric Water Lines (LMWL; Clark & Fritz 1997; Darling & Talbot 2003; Darling *et al.* 2003, Leng & Adderson 2003; Tappa *et al.* 2016).

In the present paper, we summarise isotopic results from streams, springs, fjord water and column water in the Ikka fjord area sampled over more than 25 years and compare these to former precipitation data from the Global Network of Isotopes in Precipitation (GNIP) database and to LMWL-data from other areas. The purpose of this paper is: 1) to make the stable isotope results from the Ikka fjord hydrological system available to interested parties, 2) to identify and quantify seasonal and altitude effects affecting the stable isotope composition of fresh water in the Ikka watershed and to establish a local meteoric water line and 3) to give an estimate of the uncontaminated isotopic composition of the so-called column water seeping from the submarine tufa columns in the fjord

and to determine its origin. Work is still in progress in the Ikka fjord and further isotopic data may be accumulated over the coming years.

The Ikka Project

The submarine tufa columns in Ikka fjord have been known to science since 1963, when they were first described by the Danish mineralogist Hans Pauly (Pauly 1963a). Pauly identified the tufa material to consist of a new carbonate mineral, a metastable, cold-water (< 7°C, e.g., Bischoff *et al.* 1993) hexahydrate of calcium carbonate ($CaCO_3 \cdot 6H_2O$), which he named *ikaite* after the old spelling of the name of the fjord (Pauly 1963a, b). Renewed interest in the tufa columns was triggered by material brought to Copenhagen by the biologist Henning Thing in 1994 and resulted in the first expedition to Ikka fjord in the summer of 1995. At the same time, a British diving expedition was also active in the fjord. The findings in 1995 were
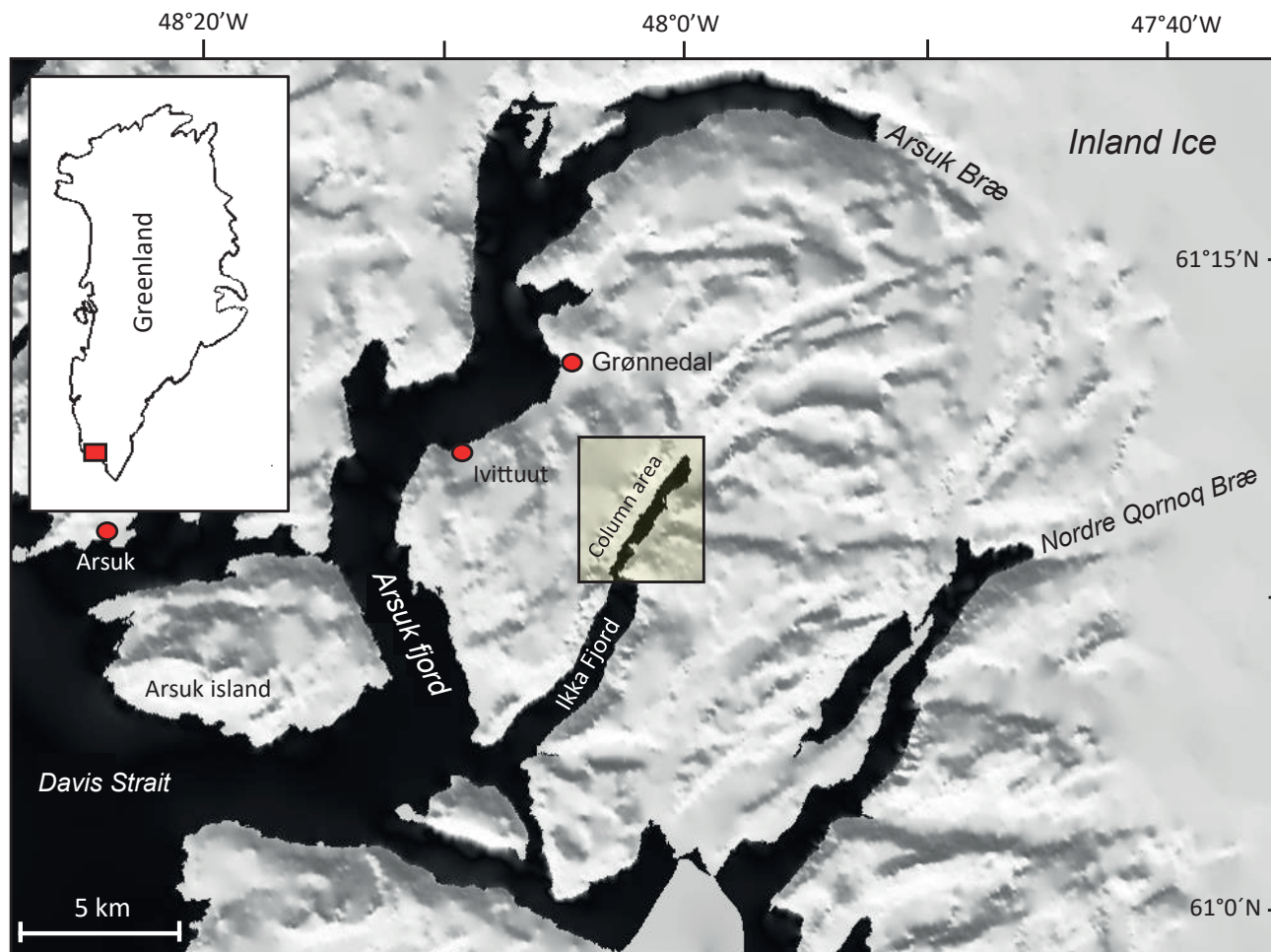

Fig. 1. Map of Ikka fjord and surrounding areas in SW Greenland. The inner part of Ikka fjord (Ikka bund) where the Ikka columns are found, is marked by a rectangle.

so promising that a major project was initiated that led to further expeditions in 1996 and 1997 including British scientists (Buchardt *et al.* 1997). During this period aspects of geology, biology, geochemistry, geophysics and hydrology were included (Kristiansen & Kristiansen 1999; Sørensen & Kristensen 2000; Petersen 2001; Buchardt *et al.* 2001; Thorbjørn & Petersen 2003; Dahl & Buchardt 2006; Stockman & Wilken 2007), and detailed mapping of the columns was achieved by aid of echo sounding and side scan sonar (Seaman 1998; Seaman & Buchardt 2006). Later, from 2006 to 2009, geological and hydrological studies were carried out in the fjord (Hansen *et al.* 2011).

Finally, from 2014 to 2022, expeditions investigated the geochemistry of the bedrock geology (Ranta *et al.* 2018; Tollefsen *et al.* 2019) and mineral alterations in the columns (Stockmann *et al.* 2022) and carried out a detailed mapping of the bottom of the fjord (Seaman *et al.* 2022). An overview of expedition periods and number of samples is given in Table 1. The fjord was visited several times in the period from 2002 to 2013 by a group of microbiologists, who sampled the columns for extremophile bacteria occupying the high pH (> 10) environment inside the columns (e.g., Stougaard *et al.* 2002; Schmidt *et al.* 2006; Vester *et al.* 2013; Trampe *et al.* 2016, 2017).
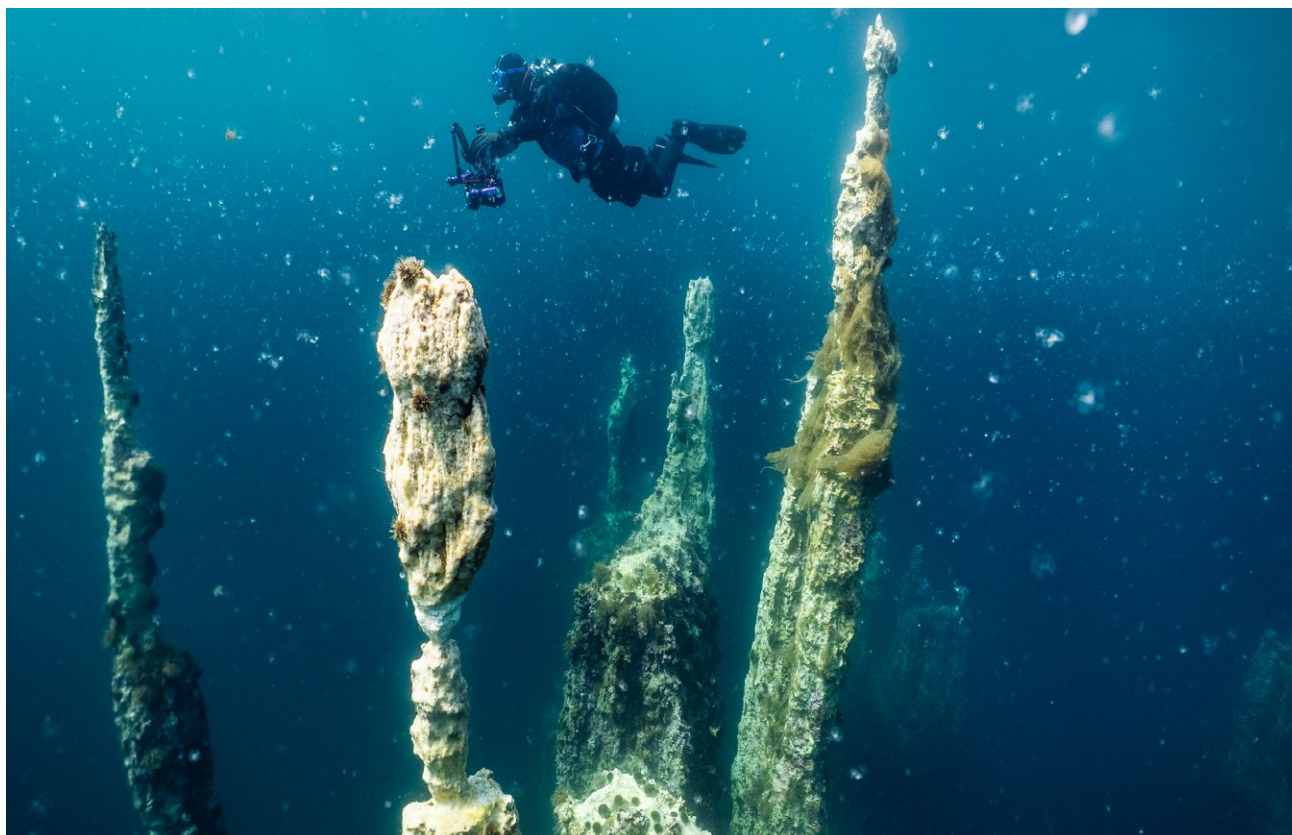
Fig. 2. Underwater photo of tufa columns from the inner part of Ikka fjord. Columns are 12 to 15 m high in this area. Note the cutting surface at the number two column from left. The column above this surface is about 1.3 m high. Columns are vertical and tilt is caused by camera distortion. Photo courtesy by Uli Kunz, SUBMARIS, 2024.

Table 1. Sampling periods and number of samples from individual water types

| Year period 1 period 2	1995 early July early Aug.	1996 mid-Aug.	1997 early Aug.	2006 mid-Aug.	2007 early July October	2018 late June	2019 late June	2021 late Aug.
n: δ^{18}O	64	99	39	33	37	10	14	9
n: δ^2H	63	66	39	0	0	10	14	9
fjord water	30	54	10	21	9	0	2	0
streams	15	16	2	1	2	1	12	5
springs	3	14	12	4	15	9	0	4
lakes	5	12	1	6	7	0	0	0
columns	8	22	14	0	3	0	0	0

Geology of the Ikka fjord area

The Ikka columns are spatially related to the Grønnedal-Íka igneous ring complex, an alkaline intrusion 8 × 3 km exposed around Ikka fjord (Fig. 3A). It consists of layered nepheline syenites intruded by a xenolithic syenite and a plug of carbonatite (Callisen 1943; Emeleus 1964; Upton 2013; Bartels *et al.* 2015). It formed during the Gardar continental rifting period from 1350 to 1125 Ma ago, when the supercontinent Columbia broke apart (Rogers & Santosh 2002). The igneous complex has a zircon age of 1325 ± 5 Ma (Stockmann *et al.* 2018a) and was intruded into Palaeoproterozoic Ketilidian gneisses (>2700 Ma), which forms the landscape in most of the Ikka fjord area (Allaart 1976). Extensive uplift and erosion took place during Palaeogene time, and major exposures of the igneous complex are found on the Randsletten plateau (500–600 m altitude) north-west of the fjord. Here, syenites, nepheline syenites, and carbonatites of sövite and ankerite compositions are common in the central part (Emeleus 1964; Ranta *et al.* 2018). Syenites are also found in a small area east of the fjord. Major

and minor dykes as well as fault systems transect the complex (Emeleus 1964). Economic interest in the iron, phosphate and rare earth contents of the igneous rocks have led to several unsuccessful prospects over the years (Bondam 1992).

Geographical and hydrological overview

The Ikka fjord (61°11′N, 48°01′W) is a submerged glacial valley that emerged from the Inland Ice cover about 11000 years ago (Weidick *et al.* 2004). It is 13 km long, up to 1.6 km wide and 170 m deep at the deepest and empties into the 500 m deep Arsuk fjord to the west over a 20 m deep sill. The fjord is flanked by 500–700 m high plateaus with steep mountain sides towards the fjord and is fringed to the north-east towards the margin of the Inland Ice by up to 900 m high mountains. It can be divided into an outer basin (Yderfjord) and an inner basin (Inderfjord) separated by a 17 m deep sill at Snævringen (the Constriction) that protects the inner
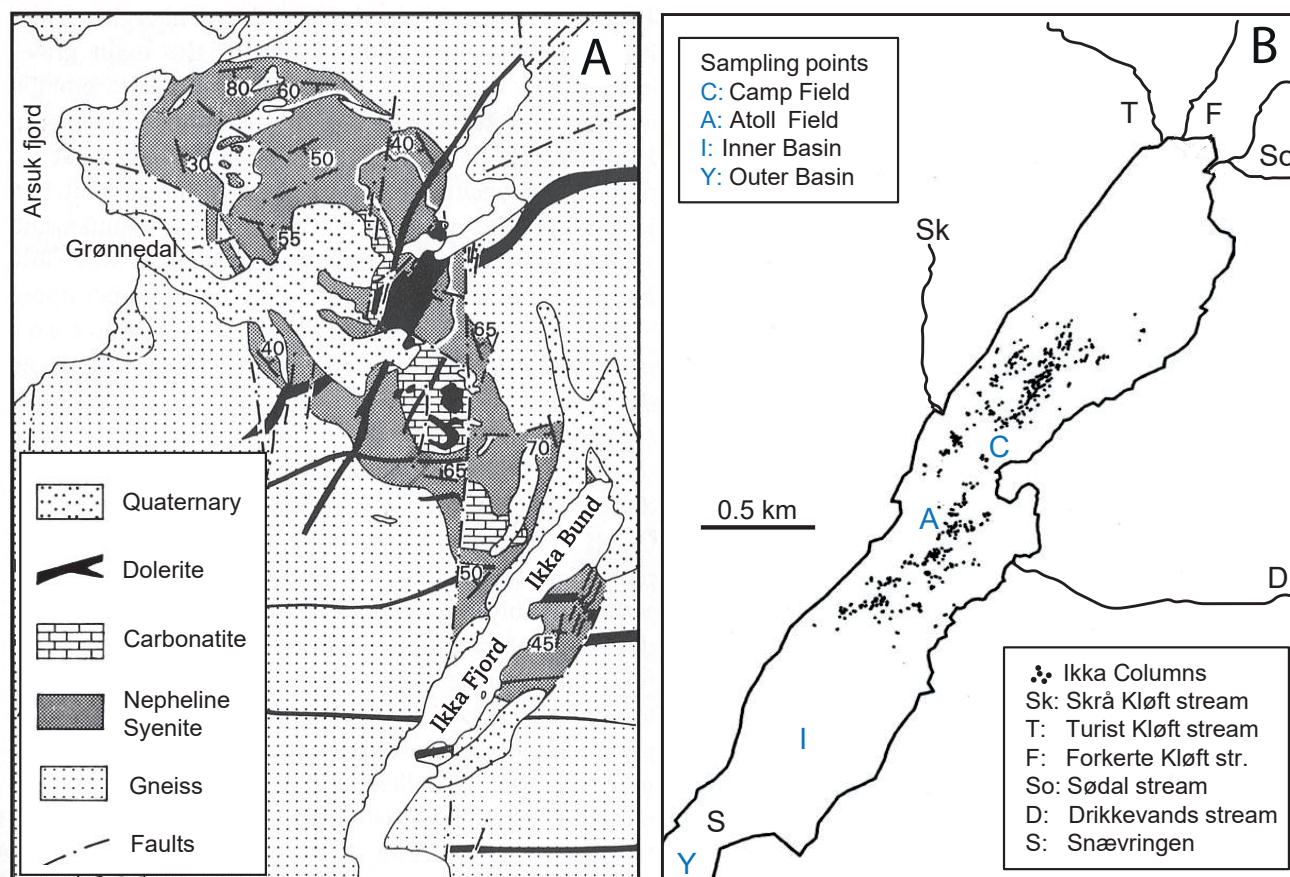
Fig. 3. A. Geological map of the Grønnedal-Íka igneous complex. Modified from Escher & Watt (1976, page 169). **B.** Map of inner part of Ikka fjord with the five sampled streams and the larger tufa columns. Also shown are sampling points for the hydrographic profiles. Modified from Seaman and Buchardt (2006) and Seaman *et al.* (2022).

part of the fjord from larger icebergs. The tufa columns are restricted to a 2 km long area in the innermost part of the inner basin (Fig. 3B; Seaman *et al.* 2022).

Annual precipitation measured at the nearby former naval base at Grønnedal (now Station Grønnedal) are between 600 and 1400 mm with a maximum in October to December and a minimum in May and June (Fristrup 1971; Hansen *et al.* 2011), and no permafrost has been detected. The area is snow-covered at least 140 days a year, and the fjord is frozen from October to May (Hansen *et al.* 2011). Mean annual air temperatures in Ikka fjord between 1961 and 2008 varied from –1.9°C in 1972 to +2.9°C in 1985 (Hansen *et al.* 2011). Bonne *et al.* (2014) gave a mean annual temperature for 2012 to 2013 from Ivittuut close to Grønnedal of +2.7°C. Later data are only available from weather stations farther south-east at Narsarsuaq airport (130 km) and Qaqortoq heliport (125 km; http:// https://www.dmi.dk/vejrarkiv. The latter gave average annual temperatures for the period from 1995 to 2021 between 0.3° (minimum) and 4.4°C (maximum) without any systematic increase over the period.

Four types of water are represented in the Ikka fjord hydrological system: fresh water, sea water, fjord water and column water. Fresh water includes streams, lakes and springs in the local catchment area. Sea water enters from the Davis Strait to the west. Fjord water is the water type formed by mixing of sea water and freshwater run-off. Column water is the highly alkaline spring water sampled by our divers from inside the submarine Ikka columns.

Five major streams named after their ravines flow into the fjord: Skrå Kløft, Turistkløft, Forkerte Kløft, Sødal and Drikkevandselv (Fig. 4; Table 2A). No effort was made to measure the discharge from the streams, but it was clear that Skrå Kløft stream had the smallest discharge and Forkerte Kløft and Sødal streams had the largest. The Skrå Kløft stream is sourced in the alkaline rocks at Randsletten, whereas the other streams all come from gneissic basement rocks. The altitude of the headwaters for the major streams varies from 900 m (Forkerte Kløft) to 300 m (Turistkløft). The catchment area for the streams discharging into Ikka fjord is about 160 km². Two glaciers drain the Inland Ice north and south of Ikka fjord: Arsuk Bræ (Arsuk Glacier, Sermeq) to the north and the Qoornoq Bræ system to the south (Fig. 1). As none of the glaciers enter the catchment area around Ikka fjord, the only source of fresh water is local precipitation.

Springs in the areas can be divided into three groups: Springs found outside the intrusive complex, springs on or around the exposures of the Grønnedal-Íka complex at the plateau at 500-metres altitude, and springs discharging at the eastern slopes of the Grønnedal-Íka complex close to the margin of the fjord. The latter springs are marked by a significant luxury of vegetation including orchids and green mosses (Fig. 12C). At least two of the springs are homothermic with all-year temperatures close to 3.4°C (Hansen *et al.* 2011). Springs at the plateau show no vegetation at all.

Lakes in the catchment area (Table 2B) are mainly found at the Randsletten plateau west of Ikka fjord at

Fig. 4. 3D-rekonstruction of the inner part of Ikka fjord and the surrounding highlands. Also shown are ravine features, where the sampled streams are flowing. Further information on streams, springs and lakes are found in Table 2.

Table 2A. Geographical data for the sampled streams, positions from Google Maps

Name Danish	Name Translated into English	Location mouth	Length (km)	Headwater altitude (m)
Skrå Kløft elv	Oblique Ravine Stream	61°11.66′N, 48°01.86′W	2.2	506
Turist Kløft elv	Turist Ravine Stream	61°12.64′N, 48°00.43′W	2.1	310
Forkerte Kløft elv	Wrong Ravine Stream	61°12.60′N, 48°00.30′W	10.4	900
Sødal elv	Lake Valley Stream	61°12.33′N, 48°00.06′W	6.3	480
Drikkevands elv	Drinking Water Stream	61°09.94′N, 48°02.14′W	1.9	470

Table 2B. Geographical data for the sampled lakes, positions from Google Maps

Name Danish	Name Translated into English	Location	Area km^2	Altitude (m)
Lejrsø	Lake Camp	61°13.15′N, 48°01.92′W		10
Xenolitsø	Xenolith Lake	61°09.94′N, 48°02.14′W	0.070	470
Tolvsøer	Twelve Lakes	61°13.45′N, 48°01.92′W	0.027	366
Øvre Radiosø	Upper Radiolake	61°12.65′N, 48°03.32′W	0.022	524
Nedre Radiosø	Lower Radiolake	61°12.62′N, 48°02.74′W	0.057	502
Wilkensø	Lake Wilken	61°12.33′N, 48°02.95′W	0.045	502
Hesteskosø	Horseshoe Lake	61°11.34′N, 47°56.40′W	1.230	470
Drikkevandssø	Drinking Water Lake	61°11.23′N, 47°58.70′W	0.008	467
Bjørnesø	Bear Lake	61°12.94′N, 48°01.79′W	0.004	490

about 500 m altitude (Radiosøerne, Xenolithsø and Bjørnesø). Tolvsøer, a shallow-water group of small lakes have been sampled at 350 m altitude north of the Grønnedal-Íka intrusion. Two major lakes (Hesteskosø and Drikkevandssø) were visited east of the fjord at 470 m altitude, and so was a small lake close to our camp site at sea level.

The fjord water is divided vertically into an upper brackish layer (salinities between 0 and 25 psu) and a deeper marine layer (salinities up to 33 psu; Fig. 5). The halocline between these two layers is typically found at depths between 2 and 5 m. The brackish layer results from mixing between sea water from Arsuk fjord and fresh water from the many streams discharging into the fjord and from precipitation directly onto the fjord and may reach temperatures up to 12°C during summer. The sea water originates from a side branch of the cold East Greenland Current which turns around the southern tip of Greenland and partly mixes with the warmer Irminger Current in Davis Strait. A tidal range of up to 3 m is responsible for exchange of water in the fjord and mixing between fresh and sea water.

Column water is the non-marine water seeping from springs at the fjord bottom into the Ikka columns, and upon mixing with the cold fjord water precipitates ikaite. Column water is a highly alkaline, sodium-carbonate brine with pH values above 10 (Buchardt *et al.* 1997; Buchardt *et al.* 2001).

Sampling

We sampled the fjord in 1995, 1996 and 1997, again in 2006 to 2007 and finally in 2018, 2019 and 2021. Activities in the fjord took place during the spring and summer seasons when the fjord was ice-free, expect for one winter expedition in April 2008. Earliest in the year were the expeditions in June and beginning of July, later expeditions were in the second half of July, August and in mid-October (see Tabel 1). Therefore – as will be demonstrated later – seasonal variations in water data are expected.

Altogether, more than 372 water samples were collected from the Ikka fjord hydrological system during the 26 years of sampling. Of these, 305 samples were analysed for ^{18}O and 201 for ^2H. The types of water samples are shown in Table 1. All samples were stored in polyethylene bottles or in vacutainers and kept refrigerated or frozen until analysis. To avoid exchange with atmospheric CO_2, samples were not filtered in the field. Local precipitation has only been sampled a few times, and precipitation data for comparison have been taken from the Global Network in Isotopes in Precipitation (GNIP) programme at Grønnedal 1961 to 1974 (Rozanski *et al.* 1993) and from Bonne *et al.* (2014).
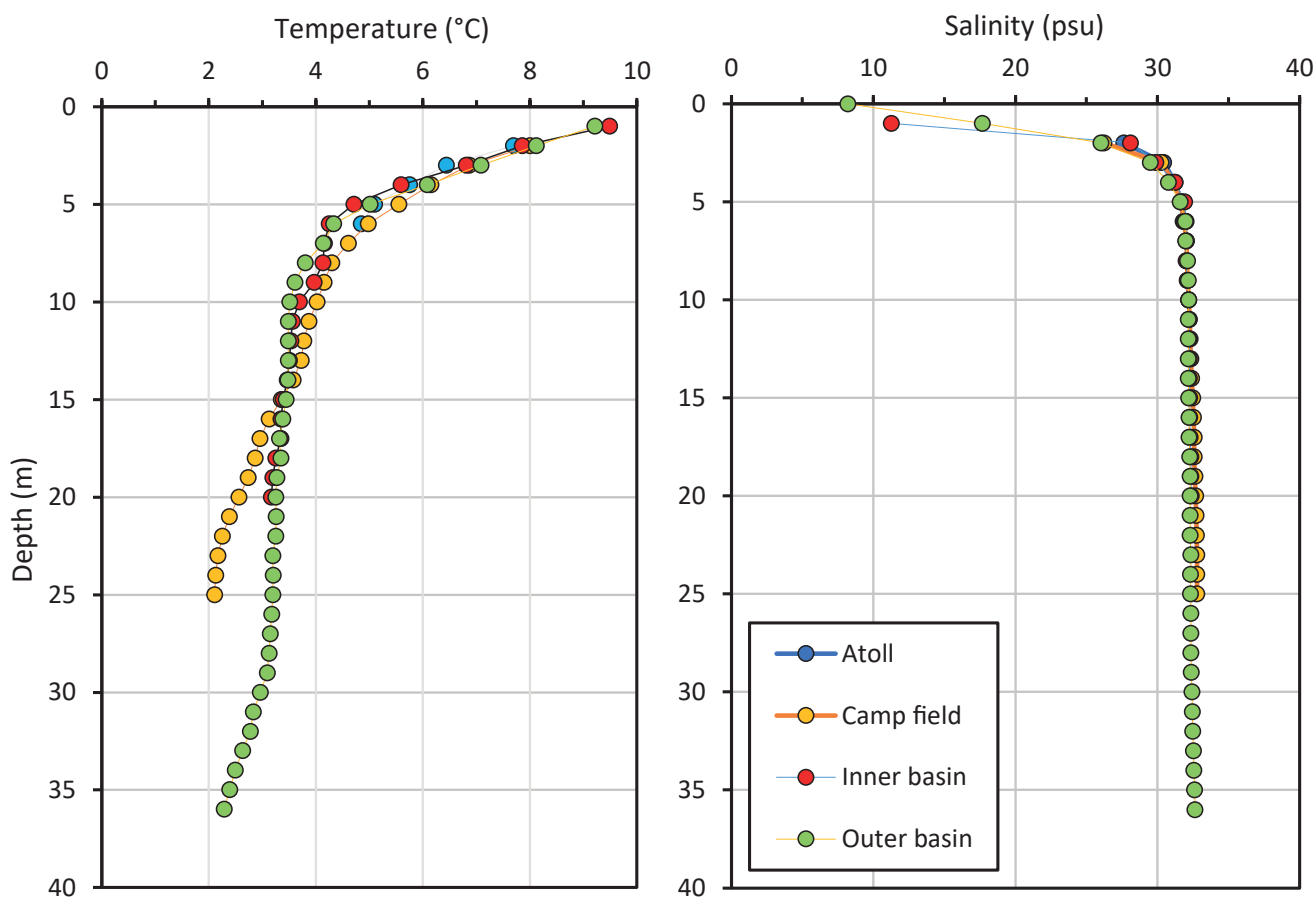
Fig. 5. Hydrographic profiles from Ikka fjord. Sampling stations refer to map on Fig. 3B. The profiles illustrate the mixing between sea water at depth and fresh water at surface. Note the marked halocline at a depth of 2 to 5 m. Data from the Danish Meteorological Institute, pers. com. (1999).

Analytical methods

The long timespan over which we have worked in Ikka fjord means that different analytical methods have been applied over the period. As an example, GPS location of sample sites has evolved from unprecise, differential determinations in 1995 (precision of ± 100 m) to highly precise modern GPS coordinates from 2005 onwards (precision better that 2 m).

Isotope analyses have been carried out by several laboratories over the years (Niels Bohr Institute and Geological Institute, both University of Copenhagen and at the Institute of Earth Sciences, University of Iceland (HÍ)) using different measuring techniques. Comparability have been achieved by application of the same international standards (V-SMOW and GISP). Hydrogen isotope ratios were determined by the zink reduction technique at 700°C on a Finnigan 250 dual inlet mass spectrometer (samples from 1995 to 2007, KU) and by H_2 equilibrium technique, using platinum sticks as catalyst on a Delta V Advantage continuous flow IRMS interfaced with a gasbench II

device (samples from 2018, 2019, 2021, HÍ). Oxygen isotope ratios were determined by the CO_2 equilibrium technique on a custom build mass spectrometer at the Niels Bohr Institute, KU (samples from 1995 to 1997), on a Micromass Isoprime continuous flow instrument at GI, KU (samples 2006 and 2007) and by a Delta V Advantage continuous flow IRMS interfaced with a gasbench II device (samples from 2018, 2019, 2021, HÍ). All results are reported as δ-values relative to V-SMOW. General reproducibility is better than $\pm 2‰$ ($\pm 1‰$) for hydrogen isotopes and $\pm 0.5‰$ ($\pm 0.1‰$) for oxygen isotopes, with numbers in brackets representing the reproducibility of the HÍ samples.

Salinity measurements of water samples were carried out in the field either by thermoconductivity sensors or by a hand-held refractometer and calibrated by conductivity measurements either in the field or later in the laboratory. Hydrographical temperature/salinity depth profiles from selected locations in the fjord system were obtained using CTD-instruments (Conductivity-Temperature-Depth). The best data sets came from a survey in July 1999 performed by the

Danish Meteorological Institute using a Seabird 9-11 sonde and from a survey carried out in 2006 (Hansen *et al.* 2011). The pH and alkalinity were measured in the field or in laboratory facilities in the nearby Ivittuut village. Concentrations of sodium, calcium and chlorine ions were measured by atomic absorption spectrometry and ion chromatography.

Results and discussion

Our water samples represent two different hydrological systems: Meteoric waters including streams, springs lakes and fjord water representing mixing between freshwater run-off and sea water. Column water samples should in principle be included in the meteoric system as spring water but will in practice be a result of mixing between pure column water and fjord water due to sampling contamination and will be treated separately. The results of the isotopic analyses are presented in Fig. 6. Individual results can be found in the Supplementary Material.

Hydrogen and oxygen isotope content of all freshwater samples have δ^2H-values between –114‰ and –84‰ and $\delta^{18}O$-values between –15.8‰ and –10.0‰ (Table 3). These values are markedly depleted in ^2H and ^{18}O compared with sea water and reflect the isotopic composition of arctic precipitation. Our freshwater samples have been collected at different
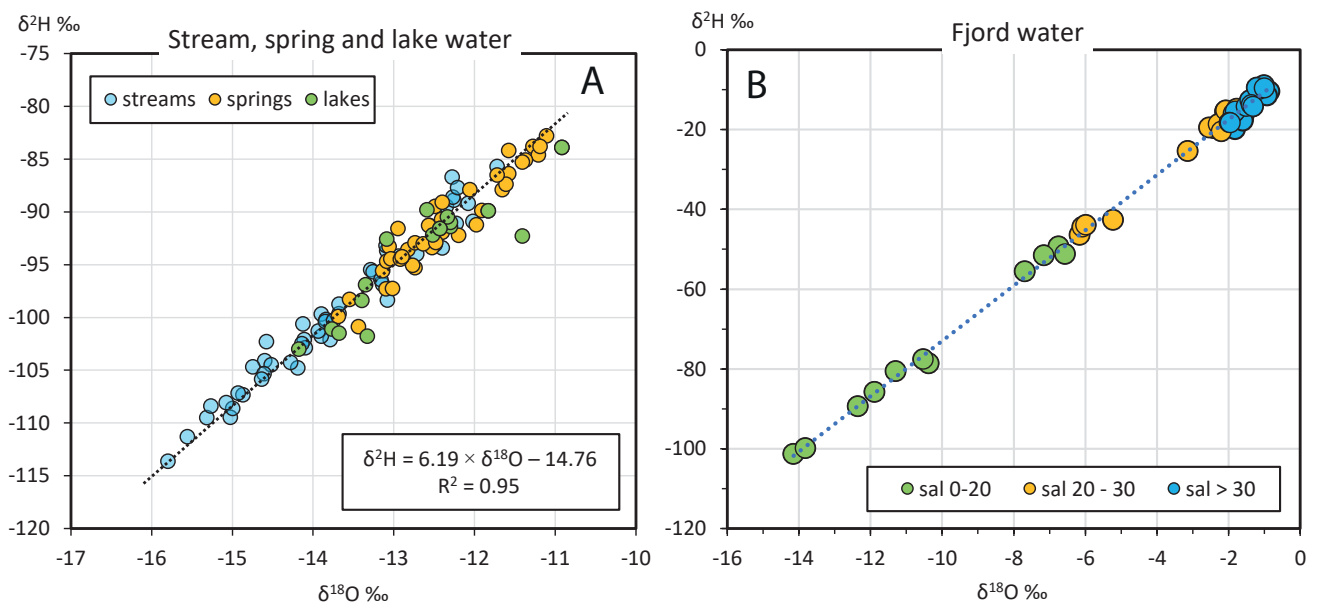
Fig. 6. δ-diagrams for hydrogen and oxygen isotope compositions of fresh water (**A**) and fjord water (**B**) in the Ikka fjord area. Note the more negative (depleted) stream water compositions compared to springs and lakes. Fjord water is divided according to salinity (sal). Green marks: above halocline, orange marks: inside halocline, blue marks: below halocline. Equations based on least square linear regressions.

Table 3. Overview of isotopic results

Type	Parameter	Precipitation*	Streams	Springs	Lakes	Fjord water	Column water
δ^2H‰	n	72	51	38	18	41	44
"	average	–94.1	–99.3	–91.5	–93.4	n.d.	–63.6
"	maximum	–53.3	–85.7	–82.8	–83.9	–8.9	–15.2
"	minimum	–133.3	–113.7	–100.9	–103	–101,3	–95.7
$\delta^{18}O$‰	n	95	55	61	31	130	47
"	average	–12	–13.7	–12.9	–12.6	n.d.	–8.5
"	maximum	–6.5	–11.7	–10.8	–10.0	–0.8	–1.9
"	minimum	–17.5	–15.8	–13.7	–14.2	–14.2	–13.4
LMWL	slope	6.34	6.56	6.37	5.58	6.93	6.96
LMWL	offset	–16.6	–9.51	–12.2	–23.2	–3.62	–2.12
LMWL	R^2	0.87	0.96	0.93	0.85	0.99	0.99

LMWL: Local Meteoric Water Line
*data from GNIP network

times of the year, and streams and springs have been sourced at varying altitudes (0 to 900 m). However, the strong correlation between the isotopic compositions of all the samples ($R^2 = 0.95$, n = 111) suggests that they belong to the same hydrological system as defined by a local meteoric water line (LMWL):

$$\delta^2H = 6.2 \times \delta^{18}O - 14.8 \text{ (least square regression)}$$

Precipitation

The strong correlation between the δ^2H- and $\delta^{18}O$-values from our freshwater samples indicates a common source, in this case local precipitation. Most precipitation in the Ikka area originates from low pressure systems in the North Atlantic either to the south-west or the south-east. Especially the winter 'south-east' gale is known for its ferocity and large amounts of snow (Fristrup 1971). To reach Ikka fjord, most precipitating clouds must pass over 500–700 m high mountain plateaus, and an orographic 'rain-out effect' on the isotopic composition (Dansgaard 1964; Clark & Fritz 1997) must be expected.

As it was not possible to sample local precipitation over a whole year, the limited precipitation data from our expeditions are of little value. Fortunately, a detailed, but rather old, database exists from the GNIP (Global Network of Isotopes in Precipitation) program,

including measurements of δ^2H and $\delta^{18}O$ in precipitation from the naval base at Grønnedal (61° 13.9´N; 48° 5.9´W). The base is located only 5 km from Ikka fjord and close to the sea and we use the data as an approximation to conditions in Ikka fjord. Precipitation was sampled from 1963 to 1970 and again from 1973 to 1974 (International Atomic Energy Agency 1969, 1970, 1971, 1973, 1975 & 1979; Rozanski *et al*. 1993). Samples were pooled monthly, but unfortunately only one year (1963) was sampled and analysed in full. Precipitation was mostly in the form of snow for at least 6 months of the year, only July and August were mostly snow-free. δ^2H-values had a range from -133‰ to -53‰ and $\delta^{18}O$-values from -17.5‰ to -6.5‰ with a small seasonal effect between less enriched values during winter (October to March) and more enriched values during summer (May to August; Fig. 7). Pure rain samples (n = 6) are enriched ($\delta^{18}O$-average = -10.4‰) as compared to snow samples (n = 27, $\delta^{18}O$-average = –12.8‰). Samples designated as both rain and snow (n = 29) fall between these values ($\delta^{18}O$-average = –11.4‰). Volume-weighted annual averages for hydrogen and oxygen isotope compositions for the whole period are –94.1‰ and –12.0‰ respectively. The small seasonal effect seen in the Grønnedal precipitation is related to its coastal climate (23 km to Davis Strait), and as all samples were taken close to sea level, any altitude effects can be excluded. Deuterium excess values
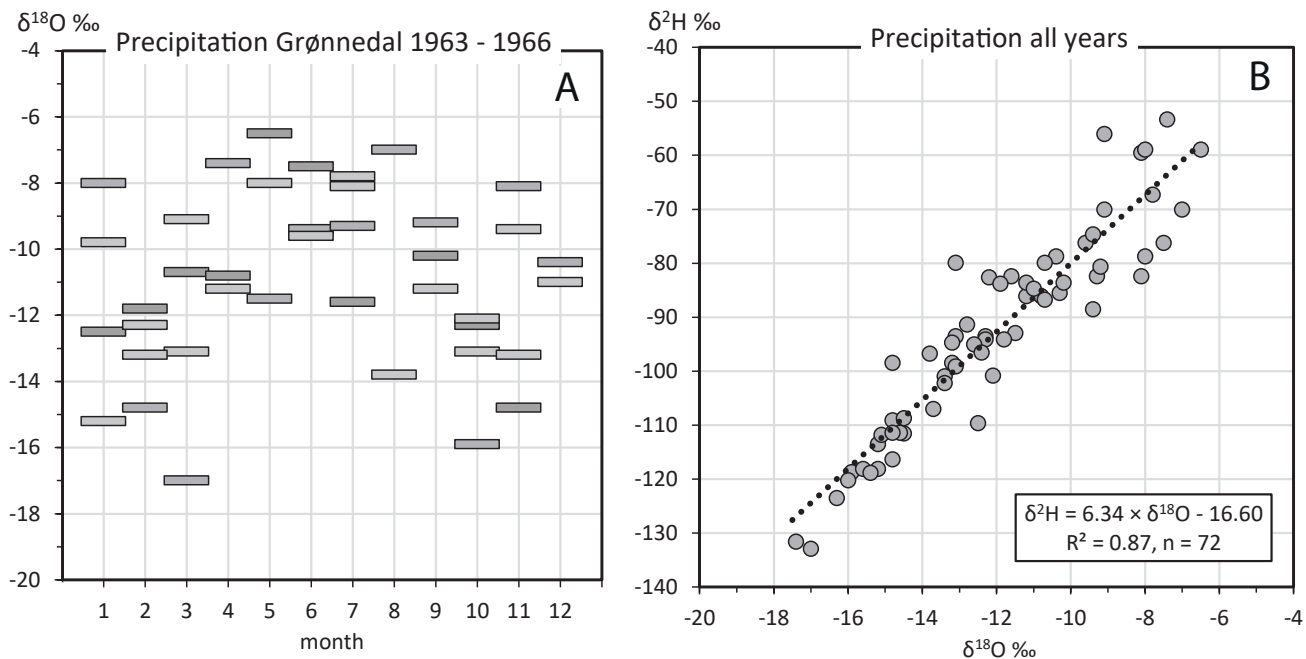
Fig. 7. Precipitation data from the GNIP-database sampled at the former naval base Grønnedal 5 km west of Ikka fjord. Left diagram: Mean $\delta^{18}O$-values for individual months for the period 1963 to 1966. Summer precipitation is more positive (enriched) in ^{18}O compared to the rest of the year, and winter precipitation has a wider range in ^{18}O composition. Right diagram; δ-relation for all precipitation samples (monthly mean) from the periods 1961-1970 and 1973 and 1974. Note the large spread in isotopic compositions. Weighted mean values for all years are –87.7‰ for δ^2H and –11.29‰ for $\delta^{18}O$. Equation based on least square regressions.

(d ‰ = δ²H – 8× δ¹⁸O; Dansgaard 1964) vary between –20‰ and +25‰ (average +2.8‰) with no relation to either amount or type of precipitation, only temperature is weakly negatively correlated with d (R^2 = 0.31). Deuterium excess in precipitation is mainly related to relative humidity (RH) at the source areas and is a measure of nonequilibrium fractionation at the sea surface. The large spread suggests varying moisture sources for the precipitation with changing RH conditions.

Since 1974 an increase in summer temperatures of about 1°C has been estimated from meteorological data (Hansen *et al.* 2011). This increase would probably lead to a minor increase in O and H stable isotope compositions of the precipitation. A later study by Bonne *et al.* (2014) includes stable isotope precipitation data from Grønnedal for a period from July 2011 to November 2012. Data from 39 samples of rain and snow have δ¹⁸O values between –20‰ and –6‰ with no mean values given. These numbers are almost identical to the older GNIP dataset.

The relationship between δ²H and δ¹⁸O from the GNIP data (Fig. 7) is defined by a local meteoric water line (LMWL) given by the equation (Table 3):

$$\delta^2H = 6.3 \times \delta^{18}O - 16.6; R^2 = 0.87; n = 72$$

This equation is biased by the incomplete dataset missing several monthly results. Taking the values from the only complete year 1963 yields a slightly different LMWL of

$$\delta^2H = 6.7 \times \delta^{18}O - 16.2; R^2 = 0.91; n = 12$$

The large differences in slope and intercept between the local GNIP-lines and the GMWL (δ²H = 8 × δ¹⁸O + 10) reflect differences in evaporative regime in the moisture source areas, also reflected in the deuterium excess variations.

Stream water

Stream water samples were collected from streams in the watershed area, mainly at sea level. Headwater altitude varied from a few metres above sea level to 900 m for the Forkerte Kløft stream (Table 2A). δ²H- and δ¹⁸O-values varied from –114‰ to –86‰ (n = 51) and from –15.8‰ to –11.7‰ (n = 51) respectively (Table 3). Mean values are –99‰ for δ²H and –13.7‰ for δ¹⁸O. Taken together, the stream data define a local meteoric water line (LMWL):

$$\delta^2H = 6.6 \times \delta^{18}O - 9.51, R^2 = 0.96, n = 51$$

A seasonal effect is evident for our stream data. Sam-ples collected from streams early in the season in June and beginning of July (1995, 2018, 2019) are depleted in both ²H and ¹⁸O as compared to later sampling of the same streams in late July, August, and October (1996, 1997, 2006, 2007 and 2021; Fig. 8). Mean δ-values for samples from the early sampling periods are –105‰ for δ²H and –14.5‰ for δ¹⁸O and –93‰ and –12.7‰ respectively for the late periods. The Ikka area is snow-covered for more than half of the year, and snow was observed on northerly facing slopes in June and early July. Thus, our early stream samples are probably dominated by melting of isotopically depleted snow from the foregoing winter, whereas the late samples reflect summer precipitation in the form of rain. The most depleted δ¹⁸O-composition of all streams (–15.8‰) were found in June 1995 in the stream Forkerte Kløft sourced at the highest altitudes in the area.

When compared, stream and precipitation (GNIP) data reveal interesting aspects. The slopes as defined from the two LMWL´s are almost identical (6.6 versus 6.3) indicating that the two sample sets belong to the same meteoric system. But the range in precipitation data is more than twice as large (δ¹⁸O: –17.5‰ to -6.5‰) as that of the stream data (–15.8‰ to –11.7‰), and the stream data – even from the late season samples – are comparable only to the more depleted values of the precipitation data.

Altitude effects

Headwaters of the streams vary from 300 to 900 m altitude (Forkerte Kløft). Samples were collected mainly at the stream mouths at sea level but are here represented by the altitude of their source areas. The altitude plot (Fig. 8) illustrates a combination of seasonal and altitude effects. Viewed individually, both early and late samples are systematically depleted with increasing altitude. An estimate of the δ¹⁸O-value of this altitude effect from linear regression amounts to between –3.1‰ (early samples) and –3.6‰ (late samples) for the 900 m difference in source areas or between –0.3‰ and –0.4‰ pr. 100 m. Whether these numbers are results of climatic conditions or reflect a true isotopic orographic effect (e.g., Clark & Fritz 1997) is unclear, but the fact that both early and late stream waters are affected in parallel, points to a general isotopic altitude-related rain-out effect. If all precipitating clouds had to cross the mountains along Ikka fjord, the orographic rain-out effect would probably lead to identical, isotopically depleted rain and snow falling on the back side in the fjord area. As this is obviously not the case, most of the precipitating cloud system must enter from the sea via the Ikka fjord valley before climbing the fjord sides. If so, precipitation from the
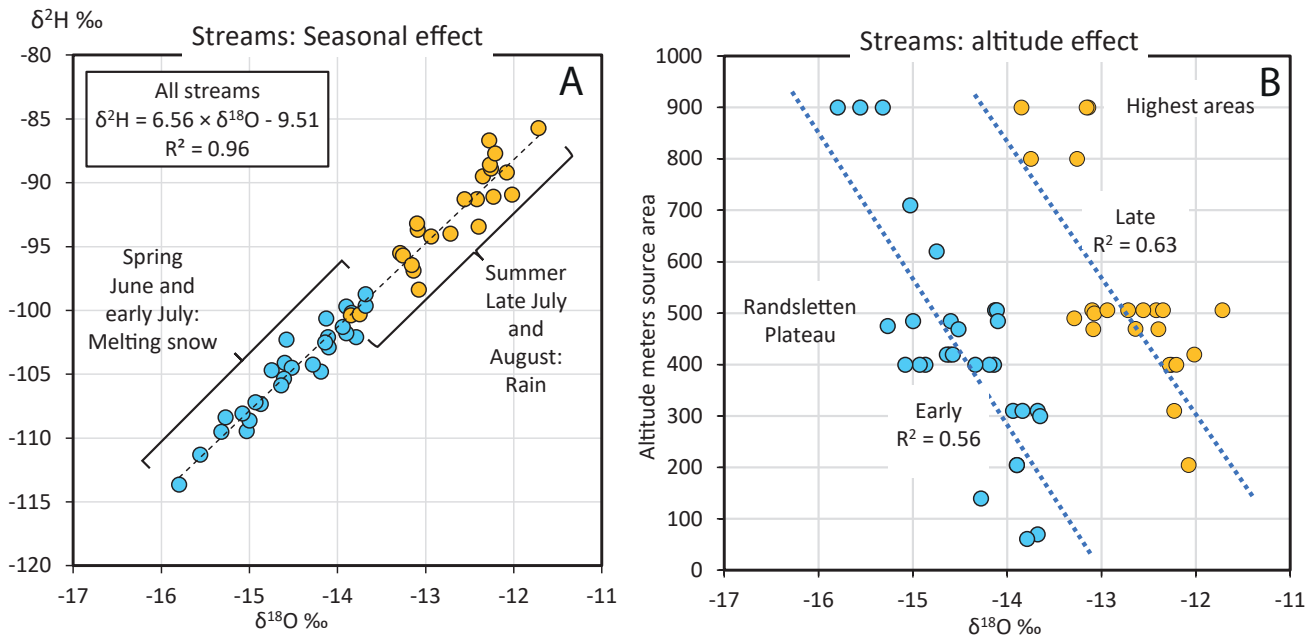
Fig. 8. Hydrogen and oxygen isotope composition data for all streams sampled at different years and from streams sourced at different altitudes. **A.** Seasonal effects in isotopic composition is obvious from differences between early and late sampling related to melting snow or rain as source. **B.** An isotopic altitude effect is suggested when data are treated separately for early and late sampling periods. Lines show linear regressions. Altitude effect amounts to -0.3 to $-0.4‰$ $\delta^{18}O$ pr. 100 m elevation.

Grønnedal area cannot be the only source of stream water in Ikka fjord.

Our calculated altitude effect of -0.3 to $-0.4‰$ $\delta^{18}O$ pr. 100 m elevation is comparable to other studies. Darling and Talbot (2003) reported values of $-0.2‰$ to $-0.3‰$ $\delta^{18}O$ from Scotland, Tappa *et al.* (2016) gave a value of $-0.22‰$ $\delta^{18}O$ for a mountainous area in Idaho, US and Clark & Fritz (1997) summarised eight studies to vary between $-0.1‰$ and $-0.5‰$ $\delta^{18}O$ pr. 100 m elevation.

Spring water

Over the study period, 61 samples were collected from freshwater springs west and east of Ikka fjord (Fig. 9A). Most samples are enriched in ^{18}O by $1‰$ to $2‰$ when compared to stream samples from the same year. 55 samples were from eight spring areas close to sea level (< 50 m altitude) at the western side of the fjord below the carbonatite and syenite exposures. This water type had our special attention as a possible source for the column water leaking from the submarine tufa towers in the fjord. Two of these springs were monitored throughout a year (August 2006 to July 2007) and proved to be homothermal with year-long temperatures close to 3.4°C (Hansen *et al.* 2011). Mean annual temperatures in the Ikka area are estimated to no higher than 2.9°C (Hansen *et al.* 2011), so extra heat must be provided for these springs, maybe from radioactive decay in the intrusive complex.

The 2400 m traverse through the eight springs along the western shoreline from Turist Elv in the north to the Skrå Kløft Elv further south (Fig. 4) showed both seasonal and lateral variations in isotopic composition (Fig. 9B). The samples from early July in 1995 were the most ^{18}O-depleted (average $\delta^{18}O$: $-13.7‰ \pm 0.1‰$), whereas the springs sampled at the same time of the year in 2007 were among the most enriched (average $\delta^{18}O$: $-11.4‰ \pm 0.5‰$). Samples from 2018 (June) and from late in the season in 1996, 1997 and 2006 (August) fall between these two extremes. Lateral variations are pronounced between the isotopically depleted springs in the central part of the traverse below the carbonatite exposures (from approx. 600 m to 1500 m, Fig. 9B) and the isotopically enriched springs outside this area, where bedrocks are either syenite or gneiss. The maximal difference amounts to $2.0‰$ $\delta^{18}O$ (1996). pH values for these springs vary from 7.1 to 8.2, Ca^{2+} concentrations from 6.0 mg/l to 41.1 mg/l and Sr^{2+} concentrations from 0.3 mg/l to 39.6 mg/l. pH values, Ca- and Sr-concentrations are highest in springs below the exposures of carbonatite, whereas the lowest values are found in the gneissic areas outside the igneous complex. It is thus obvious that the water in the springs below the carbonatite are modified by dissolution of the Ca-rich carbonatitic rocks. Sodium concentrations vary between 2.2 and 5.8 mg/L in the carbonatite-near springs and is higher than those sourced in gneiss (< 3mg/L), but significantly lower than the column water (3900 to 9100 mg/L).
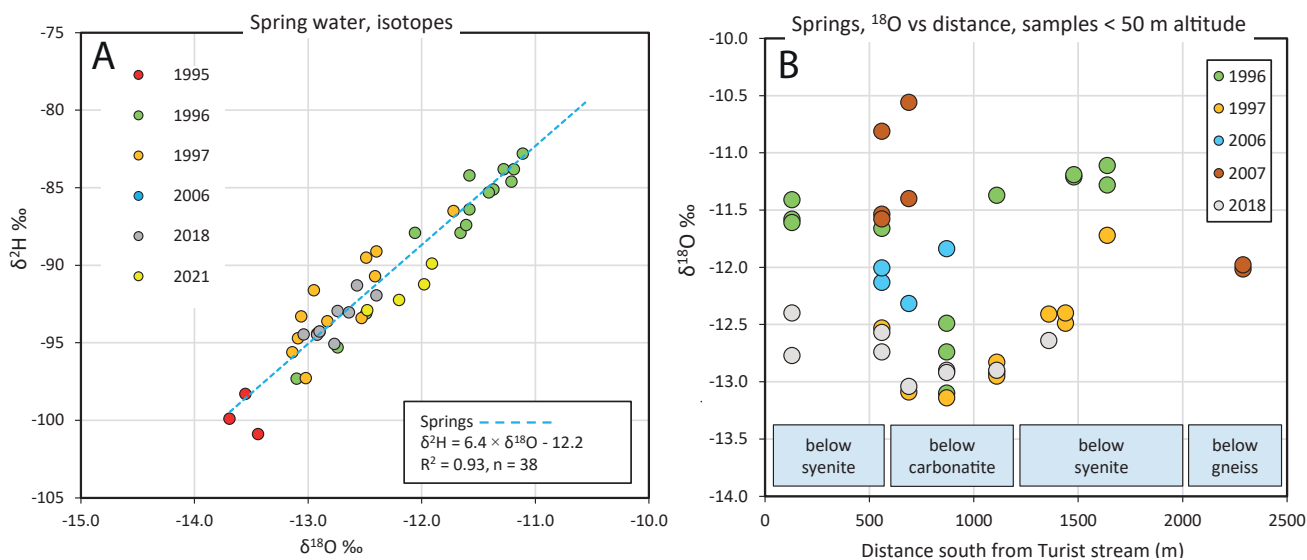
Fig. 9. Hydrogen and oxygen isotope compositions of spring water samples from all years (**A**). The diagram illustrates a seasonal effect where samples from 1995 (early July) are significantly depleted compared to later samples. Samples from 1996 (late August) are the most enriched. Equation based on least square regression. Oxygen isotope composition of spring water sampled at the foot of the igneous exposures along the west side of the fjord (**B**). Note the depletion of samples below the carbonatite. These springs are marked by a luxurious vegetation, whereas springs outside of the carbonatite are free of plants.

The large spread in the spring water isotopic compositions points to a surface-near source with a low residence time – probably local precipitation and melting snow – rather than deep groundwater from the Grønnedal-Íka complex with a more constant isotopic composition. The homothermal character of at least two of the springs below the carbonatite exposures, on the contrary, sems to indicate a deeper source for these springs. The igneous complex is characterised by numerous cracks and fissures and a higher permeability compared to the adjacent homogenic gneissic rocks, which probably result in a more complex source for the spring water below the exposures than the surface-derived water from the gneiss.

Eight spring water samples came from the east side of the fjord and from the Randsletten plateau at altitudes up to 520 m. The samples from 2007 suggest a possible altitude effect estimated to –1.5‰ for ^{2}H and –0.2‰ for ^{18}O comparable to those for the streams.

δ^2H-data are not available from spring water in the years 2006 and 2007, but the rest of the samples define a nice LMWL ($R^2 = 0.93$, n = 38) with a slope of 6.4 and an intercept of -12.2. This slope is close to that of the stream data (6.6, $R^2 = 0.96$) and Grønnedal precipitation (6.3, $R^2 = 0.87$) and demonstrate the close relationship between different components of the hydrological system in and around Ikka fjord.

Lake water

31 samples of surface water were collected from six lakes at altitudes between 350 and 520 m at the

Grønnedal-Íka plateau inside and outside the margins of the intrusion and from three lakes at the east side of the fjord at 10 and 470 m (Table 2B). Their isotopic values vary from –103‰ to –84‰ (δ^2H) and –14.2‰ to –10.0‰ (δ^{18}O; Table 3). Samples from 1995, 1996 and 1997 have been analysed for both ^{2}H and ^{18}O, the remaining from 2006 and 2007 only for ^{18}O. Most of the lake water samples fit the LMWL as defined by stream and spring data, but samples from small and shallow lakes (Bjørnesø, Tolvsøer and Camp Lake) are affected by evaporative enrichment and plot to the right of the LMWL (Fig. 10). The only lake inside the igneous complex (Xenolith Lake at 470 m altitude) is markedly enriched in calcium (Ca-concentration between 14.1 and 16.7 mg/L), magnesium and strontium reflecting the local bed rock geology. Other lakes all have calcium concentrations below 10 mg/L and down to 0.5 mg/L for lakes in the gneissic areas east of the fjord. The bedrock is also reflected in pH, which is slightly higher in Xenolith Lake than in the remaining lakes (pH = 7.9 compared to values between 6.7 and 7.5). The shallow Twelve Lakes (Tolvsøer) at 360 m altitude show a strong annual effect. The more positive oxygen isotope composition in 2006 and 2007 (δ^{18}O between –10.1‰ and –11.3‰) illustrates evaporation from the shallow lake surface in the summer period, whereas the 1995 sample (δ^{18}O = –13.3‰) taken at the same time of the year (August) must reflect input of local, depleted precipitation. The few data define a local evaporation line LEL with a slope of 5.6. A comparable study from Kangerlussuaq/Søndre Strømfjord (Leng *et al.* 2003) 650 km to the north in Greenland

Lakes: ^{2}H vs. ^{18}O

streams
$\delta^2H = 6.56 \times \delta^{18}O - 9.51$
$R^2 = 0.96$

Streams

Lakes

lakes
$\delta^2H = 5.58 \times \delta^{18}O - 23.2$
$R^2 = 0.85$
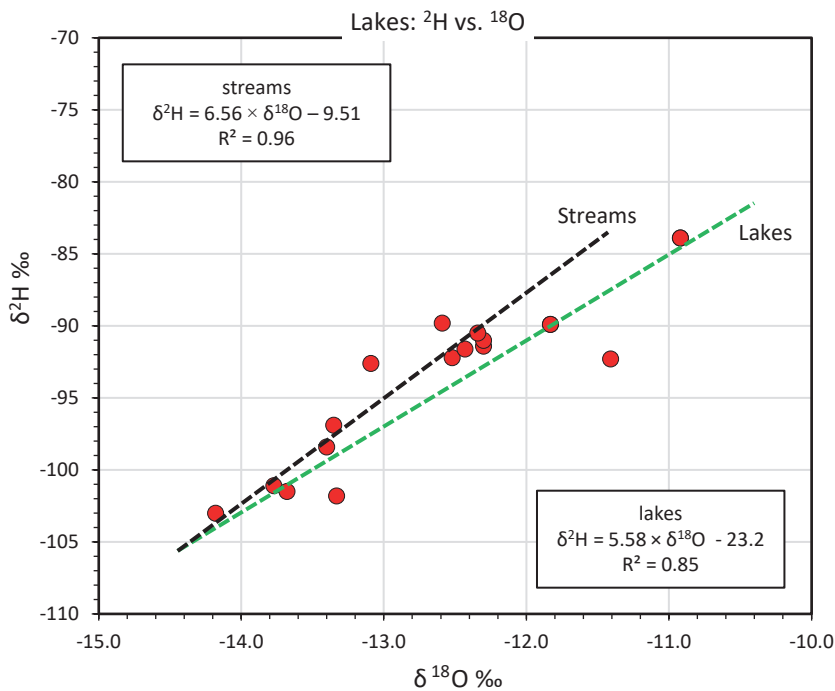
Fig. 10. δ-diagram for lake water samples mainly from the 500 m plateau west of Ikka fjord. Most enriched samples are from small lakes affected by evaporation. Lake samples define a linear regression line LEL with a smaller slope than the shown line for streams caused by preferential evaporation of ^{2}H.

demonstrate similar evaporative effects in small lakes with LEL's lines defined by slopes between 3.9 and 5.8, highest values for the most coast-near lakes.

Fjord water

131 samples from 1995 to 1997, 2006, 2007 and 2019 were measured for ^{18}O-composition and salinity. Of these, 41 samples were also measured for δ^2H. Salinity and δ^{18}O are highly correlated ($R^2 = 0.98$). This correlation reflects the mixing system between sea water from Davis Strait and fresh water from streams and precipitation. When separated into sampling years, an even higher correlation is seen for each individual mixing system ($R^2 > 0.99$; Fig. 11). The varying slopes of the regression lines points to the fact that the end-member compositions of both fresh water and sea water differ from year to year. The 1995 correlation represents samples taken early in the season in early July, whereas samples from 1997 and 2006 were collected in August. When extrapolated to a salinity of 0, the calculated freshwater end member from 1995 has the most depleted δ^{18}O-value of –14.8‰, whereas the 2006 system shows the most enriched δ^{18}O-value of –13.2‰. The 1996 value falls between these with a δ^{18}O of -13.9‰. It has already been demonstrated how the two major streams entering the fjord early in the season are depleted by 1 to 2‰ in ^{18}O as compared to the late season. These compositions are comparable to the calculated values above.

The stratification of the fjord water column at a halocline between 2 and 5 m depth is nicely illustrated in Fig. 5. Surface water between 0 and 2 m depth has

a large spread in both salinity and δ^{18}O. The most enriched surface waters are from samples taken in the outer basin with salinities of 24.6 psu and δ^{18}O-values at –4.6‰ representing only limited mixing with fresh water, part of which probably originated as direct precipitation. Most depleted surface samples have δ^{18}O-values between –13‰ and –14‰ close to that of the streams. Water samples from within the halocline have salinities between 20 and 33 psu and δ^{18}O-values between –4‰ and –1‰. Samples taken below the halocline are all enriched in ^{18}O (δ^{18}O > –2‰) compared to the water masses above and reflect sea water composition.

The sea water entering Ikka fjord is a blend of Polar Water from the cold East Greenland Current and Atlantic Water from the Irminger Current (Buch 1995, 2002). The East Greenland Current originates in the Polar Basin, turns around Cape Farewell and follows the SW Greenland coast northwards and is characterised by salinities below 34 psu, temperatures below 2°C and is depleted in ^{18}O (δ^{18}O as low as –2‰, e.g., Azetsu-Scott & Tan 1997). The warmer Irminger Current originates in the North Atlantic Ocean and has salinities above 34.8 psu, temperatures around 4°C and is enriched in ^{18}O (δ^{18}O > 0‰, Frew *et al.* 2000). The two water masses merge along the south-west coast of Greenland, and the varying seawater compositions observed in Ikka fjord may well relate to this. It is noteworthy that the year 1995 was characterised by extraordinary large amounts of polar sea ice outside the SW Greenland coast as reflected in the Polar signature of the water in Ikka fjord (Fig. 11).
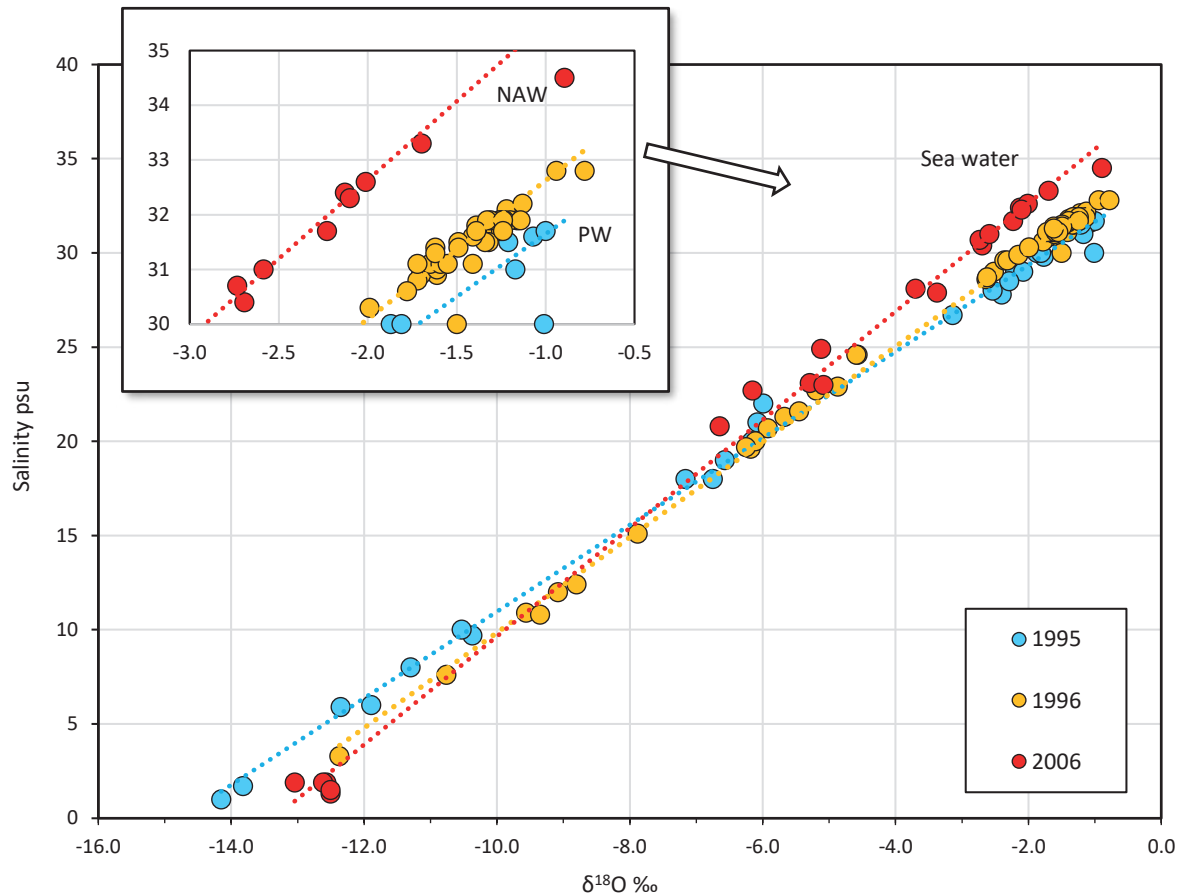
Fig. 11. Salinity/δ¹⁸O diagram showing the variable end members of the seawater/freshwater mixing system. Inserted is an enlargement of the high-salinity part of the plot. Samples from 2006 are closer to the composition of North Atlantic Water (NAW) in the Irminger Current, whereas samples from 1995 and 1996 are influenced by Polar Water (PW) in the East Greenland Current. The year 1995 was characterised by heavy packing of polar ice in Davis Strait.

It is thus not possible to determine a single salinity/δ¹⁸O value-set for the seawater component entering the fjord. Highest salinity values are between 32.8 and 33.3 psu at depths between 25 and 50 m, and corresponding δ¹⁸O-values are from –1.7 to –0.8‰. These numbers are taken as best approximations to the local seawater composition.

A smaller number of fjord water samples (41 from 1995, 1997 and 2019) were analysed for hydrogen isotope composition. The combined isotope data define the mixing line between fresh water and sea water described by the equation (Fig. 6, Table 3):

$$\delta^2H = 6.93 \times \delta^{18}O - 3.62, R^2 = 0.99, n = 41$$

Water samples with higher salinities but 'normal' ¹⁸O-concentrations were collected from deeper parts of the inner fjord. These salinities probably reflect 'freezing-out' and brine formation during winter (Bauch *et al.* 2010; Granskog *et al.* 2011). A sample from 100 m depth close to the bottom in the Yderfjord gave surprisingly low values for both salinity (29.6 psu) and oxygen isotope composition (δ¹⁸O = –2.3‰) probably caused by freshwater seeping from bottom springs. Seaman *et al.* (2022) reports pockmarks after submarine springs in the same area.
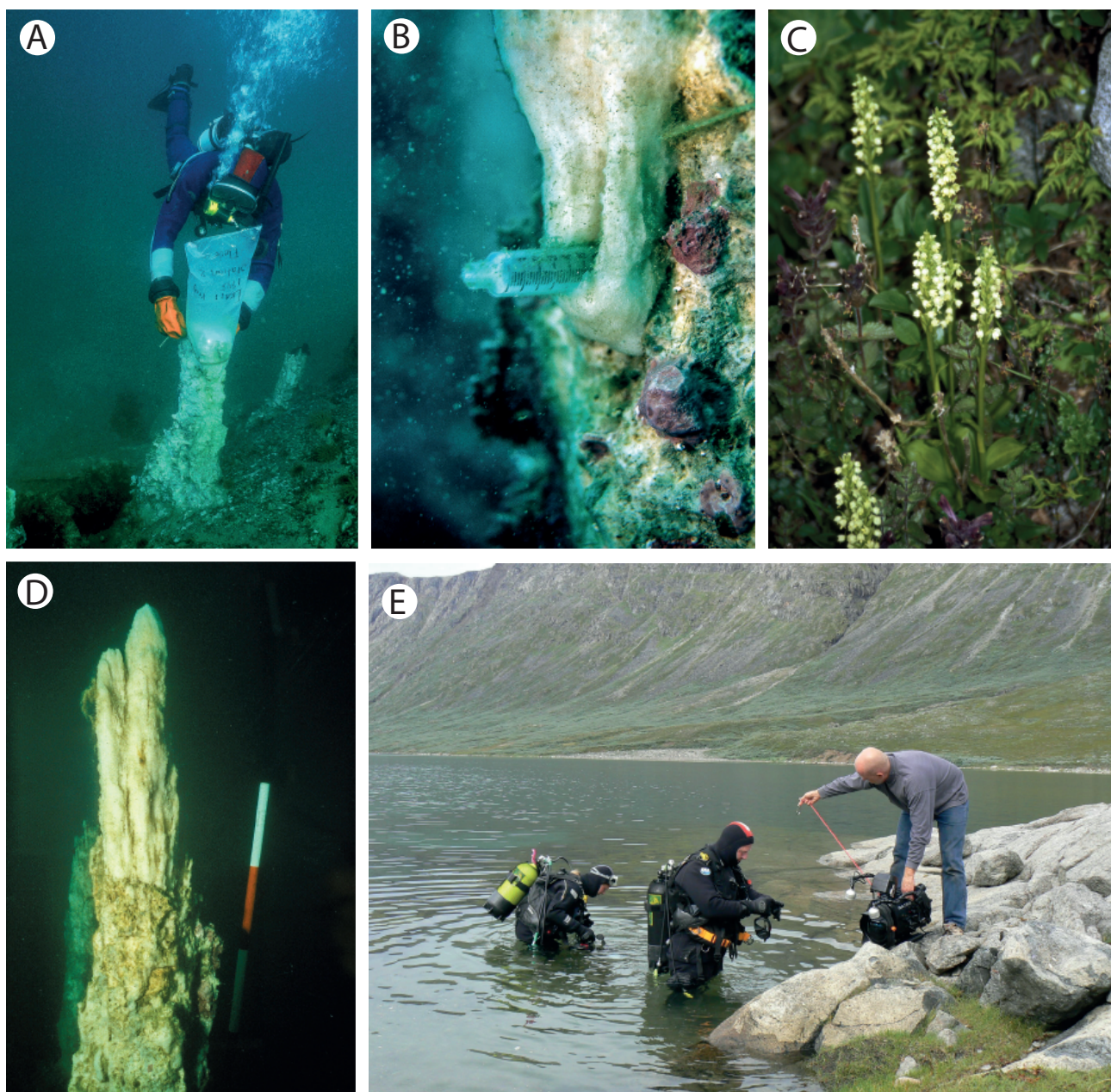
Column water

This water type is characterised by high carbonate alkalinity (up to 200 meq/L), high pH (up to 10.5), high sodium concentration (up to 6000 mg/L), and depleted hydrogen and oxygen isotope compositions (Buchardt *et al.* 2001). The working hypothesis (Pauly 1963a; Buchardt *et al.* 1997, 2001) for the growth of the submarine Ikka columns is derived from the fact that columns are restricted to the area where the Grønnedal-Íka complex is exposed around the fjord. It was suggested that a confined aquifer under the bottom of the fjord is sourced by precipitation on the 500 m high plateau formed by the Grønnedal-Íka complex west of the Inderfjord. This precipitation dis-

solves carbonates from the carbonatites and sodium from primary and secondary Na-minerals in the syenites (e.g., nepheline) within the alkaline igneous complex and becomes saturated in sodium carbonates (Bondam 1992; Buchardt *et al.* 2001; Ranta *et al.* 2018; Tollefsen *et al.* 2019; Aðalsteinsdóttir 2021). This soda-rich ground water enters the floor of the fjord as submarine springs and precipitates ikaite immediately upon mixing with the cold, calcium-rich fjord water.

As the spring water has a lower density than the fjord water, it percolates upwards and leads to growth of the columns. Precipitation of other carbonate minerals is inhibited by high phosphate concentration in the column water (Bishoff *et al.* 1993; Buchardt *et al.* 2001) and by magnesium in the sea water (Stockmann *et al.* 2018b; Tollefsen *et al.* 2018). The metastable ikaite will eventually recrystallise to monohydrocalcite, aragonite, and calcite and thus destabilise the delicate ikaite

Fig. 12. Photos from Ikka fjord. **A.** The 'bag sampling' method applied by the divers in 1995. **B.** A tapping point drilled into the column in 1996, sample water was pumped out of the column by a syringe handled by the diver. Note the fresh precipitation of ikaite minerals around the tapping point, which was inserted the year before. **C.** Example of impressive vegetation at springs below carbonatite exposure, here orchids (*Psedorchis straminea*). **D.** Column showing a year's growth (appr. 50 cm) over cutting surface. **E.** Divers preparing for a dive in the fjord. Photos by Richard Martin, Gabrielle Stockmann and Bjørn Buchardt.

structure (Dahl & Buchardt 2006; Hansen *et al.* 2011; Stockmann *et al.* 2022).

Sampling of the column water was carried out by scuba divers, and fjord water contamination was a major problem. Sampling stations were placed at columns between 8 and 10 m water depth, where the surrounding fjord water had salinities higher than 25 psu and $\delta^{18}O$-values more positive than –2‰. In 1995, column water was sampled in plastic bags tied above cut columns, so-called bag water (Fig. 12A). This water was clearly contaminated by fjord water (visible precipitation of ikaite inside the bags), but nevertheless demonstrated that column water had a lower density, and much higher pH and alkalinity than the surrounding fjord water. The following years (1996 and 1997), the sampling method was improved by placing tapping ports in drilled holes sealed with linseed puddy in the columns and sucking water out with syringes (Fig. 12B). Two 'tapping stations' were established: The Atoll Station at 10 m water depth close to the so-called Atoll structure (12 samples), and the Camp Field Station at 8 m depth close to the camp (11 samples). By this method samples of column water with only minor fjord-water contamination could be collected.

In 2007, sensors were placed inside a column at the Camp Field Station to monitor pH-, temperature- and conductivity variations over a full year (Hansen *et al.* 2011). Data indicated a long stabilisation period of more than three months before constant values were obtained. Finally, pH settled around 10.3 and conductivity at 6.9 mS cm⁻¹ (~ 6.7 psu at 3°C). These values were considered to represent the uncontaminated

column water (fjord water in contact with the columns had pH of ~ 8 and conductivity of 31 mS cm⁻¹ or 33.2 psu). The long stabilisation period for the pH-sensors makes it unlikely that our syringe samples reflect totally uncontaminated column water.

The stable isotope plot (δ^2H vs $\delta^{18}O$) of column water illustrates the effect of fjord water contamination (Fig. 13). δ^2H- and $\delta^{18}O$-values are highly correlated ($R^2 = 0.99$) because of simple two-component mixing between fjord water and the uncontaminated column water at the sampling points. The linear relation between fjord water and column water as seen in the isotope diagram allows us to calculate the percent of fjord water contamination. Our bag water samples were strongly contaminated (from 55% to 95%), and even the syringe samples contained varying amounts of fjord water (up to 55%) although most samples had less than 20% contamination.

Chemical analyses were carried out to help identify the composition of fully uncontaminated column water. pH was determined for all column water samples and varied between 8.4 pH units for the most fjord-water contaminated samples and 10.5 pH units for the least contaminated samples, whereas pH for the fjord water at the sampling points varied between 7.6 and 8.2. pH seems to stabilise at values of between 10.0 and 10.5 in samples with less than 40% contamination (Fig. 14A). Alkalinity was measured in 14 column water samples (Fig. 14B). Syringe water had the highest alkalinity and varied between 115 and 200 meq/L, bag water had values between 25 and 64 meq/L reflecting the fjord water contamination, whereas fjord water had very low alkalinity (as expected) of 2 meq/L. In
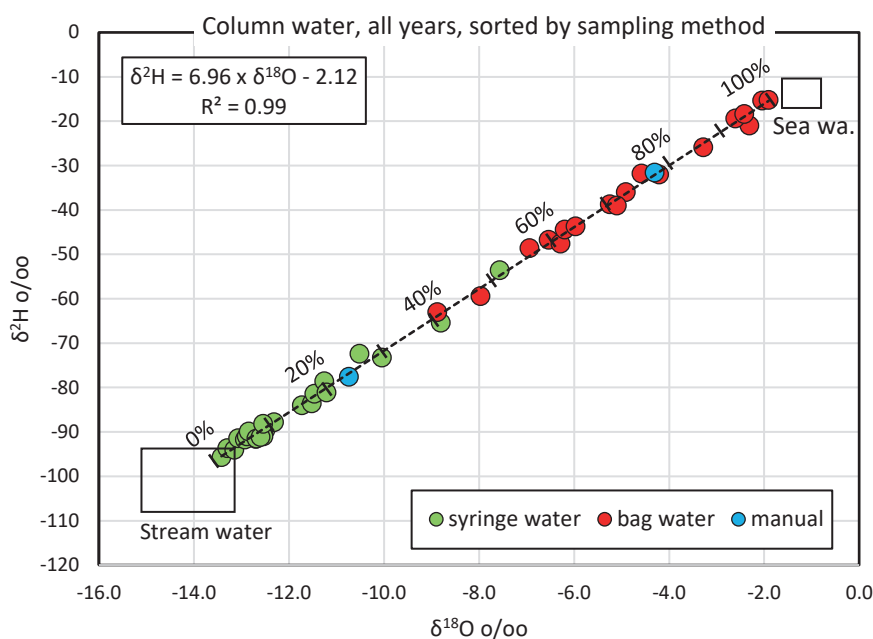
Fig. 13. δ-diagram for column water sampled underwater by different methods. Contamination by sea water during sampling is most pronounced for the bag water, but also water sampled by the syringe method was contaminated to varying degrees. The figure illustrates a simple percentage calculation for the seawater contamination.
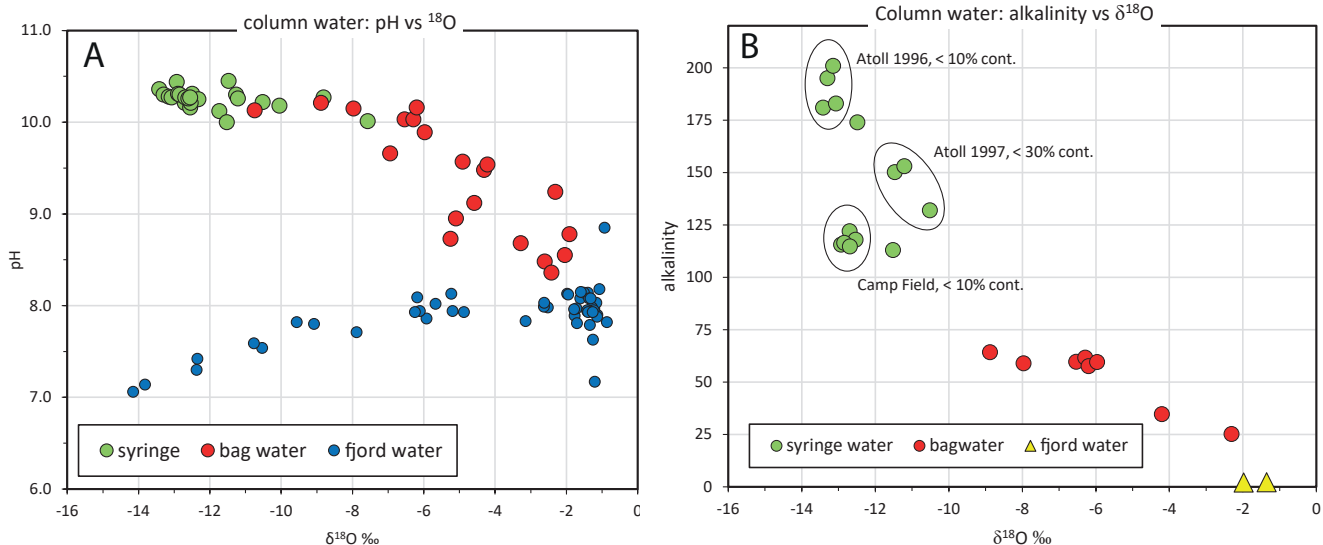
Fig. 14. pH (**A**) and alkalinity (**B**) of column water sampled by the different methods plotted against their δ¹⁸O-values. All samples were collected at depths below 8 m. Also shown are the pH-values of fjord water samples ranging from fresh water to sea water. Note the difference in alkalinity for least contaminated water samples from the two sampling stations.

contrast to pH, alkalinity seems to vary between the two sampling stations, even at contaminations less than 10%. Thus, Atoll samples from 1996 were significantly higher in alkalinity (between 180 and 200 meq/L) than Camp field samples (110 to 122 meq/L) probably reflecting true differences.

If the column water originates as precipitation on the Grønnedal-Íka Complex, then its chloride ion concentrations should be neglectable as shown by several analyses of stream and spring water from the complex (all < 0.03 Cl⁻ mg/L), and no chloride-containing minerals are known from the igneous complex. Thus, chloride ion concentration in column water is a direct measure of fjord water contamination. Column water samples with estimated less than 10% contamination still contain between 750 and 2150 mg/L of chloride ions. The chloride ion concentrations define a linear mixing system between low Cl⁻ samples from columns and high Cl⁻ samples from the fjord (R² = 0.88, Fig. 15A). If this mixing line is extrapolated to a Cl⁻ value of zero, the corresponding δ¹⁸O-value is –14.18‰. A similar argument can be used for magnesium, and an uncontaminated δ¹⁸O-value based on Mg²⁺ concentrations come to –14.11‰. These values let us estimate a general δ¹⁸O value for the uncontaminated column water of approximately –14.2‰, slightly more negative that the least contaminated samples (–13.4‰, Atoll St. and –12.9‰, Camp St.) and the value given by Buchardt *et al.* (2001). A simple percentage calculation between fjord water composition and the suggested uncontaminated column water composition yields a contamination of 4% and 9% for these two samples.

Using the relation (LMWL) between δ¹⁸O and δ²H in column water samples, the hydrogen isotope composition of uncontaminated column water is estimated at δ²H = –102‰.

Calcium concentrations stay low in the sample water up to a contamination of at least 75% (Fig. 15B) because of ikaite precipitation in the sample containers. This level represents the end-point of ikaite precipitation (saturation), and more contaminated samples have rapidly increasing calcium concentrations up to fjord water levels of more than 300 mg/L. Strontium behaves in a similar way, as strontium ions from the fjord water (8 to 10 mg/L at 10 m depth) are incorporated into the ikaite crystals.

When the new estimate of the oxygen isotope composition (δ¹⁸O = –14.2‰) of the column water is compared to our stream data, it is evident that its depleted composition is only matched by the most depleted stream data from altitudes above 400 m. This water is likely derived by melting of winter snow on the Ikka plateau. Winter precipitation at Grønnedal (GNIP 1963 to 1974) falling as snow reached δ¹⁸O-values as low as –17.5‰. It is also clear that the surface spring water described above belong to another water type as defined by its much more enriched oxygen isotope composition and low pH and alkalinity. The present data thus support the original hypothesis that column water is sourced by precipitation falling on the top of the Grønnedal-Ika igneous complex but provide a better estimation of the composition of uncontaminated column water than those of Buchardt *et al.* (2001). No dating has been obtained for the column water, but
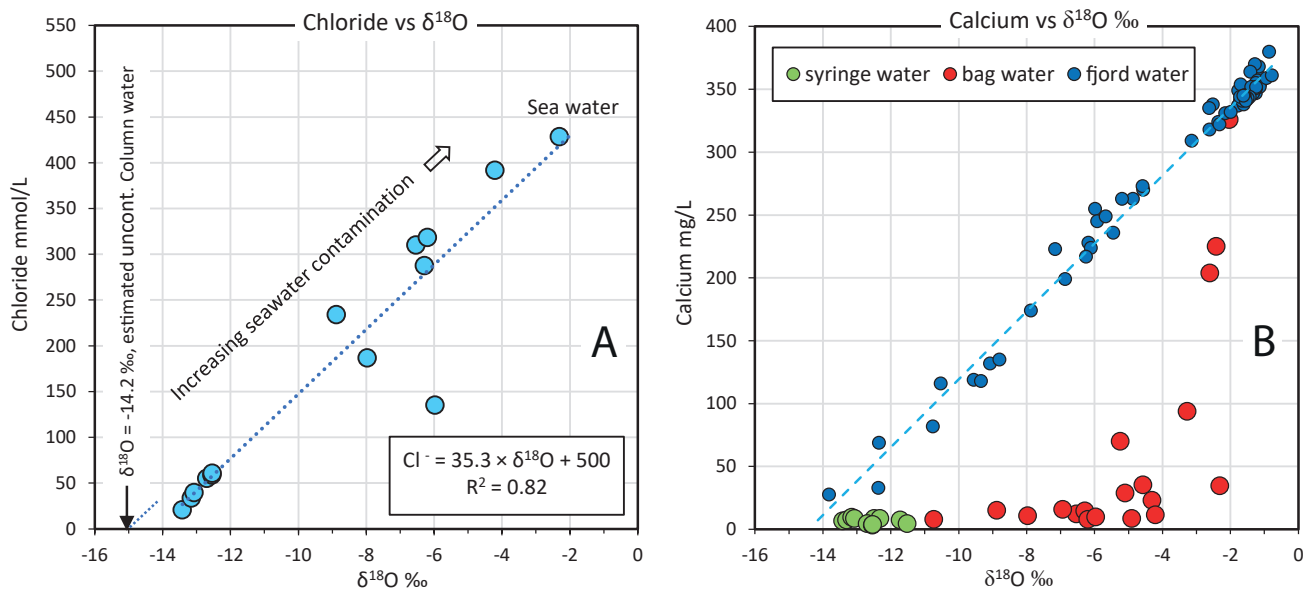
Fig. 15. Chloride ion concentration plotted against oxygen isotope composition for column water samples (**A**). Extrapolation of the linear regression line for the chloride/δ¹⁸O relation leads to a δ¹⁸O-value for chloride-free column water of –14.2‰. This value is taken as representing uncontaminated column water. A similar diagram as Fig. 14A for calcium concentration (**B**) illustrates the extraction in the sample containers of calcium ions by ikaite precipitation following mixing of calcium-free column water and calcium-rich fjord water at the sampling sites.

the large altitude difference between source and outflow (~ 500 m) suggests a long residence in cracks and fissures in the igneous complex, probably of several hundred years, and the depleted isotopic composition may well reflect lower air temperatures (Little Ice Age?) at the time of precipitation.

Temporal effects

Our sampling was continued intermittently over a 27-year long period from 1995 to 2021 and temporal effects should be expected. It is evident from our freshwater data that seasonal isotopic effects do exist in the Ikka fjord hydrological system. Streams, springs and lakes sampled early in the summer in June and early July are depleted in ²H and ¹⁸O by 14‰ and 2‰ respectively as compared to samples from late July and August. The catchment area for the Ikka fjord freshwater is not affected by meltwater from the ice cap to the east, so local precipitation – either as snow or rain – is the only source. In the Ikka area, snow was seen to persists at the higher altitudes (above 200 m) into early July but had disappeared totally in late July and August. Therefore, melting of isotopically depleted snow early in the summer can easily account for the data. Later in the summer, all precipitation falls as rain enriched in stable isotopes.

Hansen *et al*. (2011) estimated there had been an in-

crease in summer temperatures in Ikka fjord of 0.1°C per decade since 1960, and Seaman *et al*. (2022) reported water temperatures in June 2019 of 6.0° at 13 m depth close to the Atoll structure. Similar measurements in 1995 gave temperatures between 2°C and 3°C. This suggests a pronounced warming of the fjord. As the ikaite mineral is unstable at temperatures above 7°C and dissolves into water and monohydrocalcite, aragonite or calcite (Bischoff *et al*. 1993; Dahl & Buchardt 2006), a continuing warming trend might endanger the survival of the columns.

However, new CTD measurements of the Inderfjord in the summers of 2021 and 2022 combined with continuous temperature recording using a HOBO datalogger in June to August 2021 showed that the warmer (6–9°C) water of 2019 had been exchanged with colder sea water although the top part of taller columns was still exposed to > 7°C (Stockmann *et al*. 2022). None of our isotope data seem to indicate any temporal shift related to increasing temperatures in the fjord area. Climate data from nearby Narsarsuaq and Qaqortoq towns 130 km to the south-east (generated by the Danish Meteorological Institute, https://www.dmi.dk/) do not indicate any significant increase in mean annual temperatures in the area over the 27 years study period. Thus, the higher water temperatures reported by Seaman *et al*. (2022) cannot be explained by a general warming in southern Greenland. Stockmann *et al*. (2022) ascribed the seawater heating of 2019 to the

topographical complexity of the Inderfjord with narrow pathways for sea water in between columns and submarine sills combined with a strong stratification of heated freshwater on top, which requires strong gales from a specific wind direction to exchange the sea water in the Inderfjord.

Summary and conclusions

In this study, we publish hydrogen and oxygen isotope data for a full hydrological cycle including precipitation, lakes, streams and springs flowing into a fjord system, and waters formed by mixing between fjord water and sea water (Table 3). The study deals with a low-Arctic hydrological system not investigated before and covers a period over 27 years, and therefore should provide some new insights.

1) The similarity between the ^{2}H/^{18}O-relations (Table 3) for the different freshwater types demonstrate that they all belong to the same meteoric water system as shown by the high correlation ($R^2 = 0.95$) between their isotopic compositions as defined by a Local Meteoric Water Line (LMWL):

$$\delta^2H = 6.19 \times \delta^{18}O - 14.76$$
$$(n = 114, \text{ least square regression})$$

This relationship is significantly different from the GMWL (slope of 8) as defined by Craig (1961).

2) Precipitation data are only available from the GNIP-program between 1961 and 1974 sampled at the former Naval Base at Grønnedal. The data show a large spread in both δ^2H- and δ^{18}O-values with weighed annual means of –87.7‰ and –11.29‰ respectively and fit a LMWL with slope identical to our stream data.

3) The isotopic composition of stream water is affected by seasonal differences in precipitation and by source altitude. Samples collected in the early field seasons (June to early July) are depleted in ^{2}H by about 14‰ and ^{18}O by about 2‰ when compared to the late field seasons (late July and August). This effect is related to melting of isotopically depleted winter snow and should be considered when comparing data from year to year. Streams sourced at high altitudes are also depleted as compared to streams sources close to sea level, probably reflecting an orographic rain-out effect. This depletion amounts to between –0.2 and –0.3‰ δ^{18}O pr. 100 m elevation.

4) Spring water is likewise influenced by seasonal variations, the largest δ^{18}O-difference between samples from 1995 (early July) and 1996 (late August) being more than 2.5‰. Moreover, springs below the carbonatite outcrops at the north-western slopes of the fjord are depleted by 1 to 2‰ δ^{18}O (melting snow) and enriched in calcium as compared to those outside the intrusion. The large differences from year-to-year point to a shallow source for the springs. Springs below the carbonatite outcrops are not the source for the Ikka Column water.

5) Lake waters demonstrate evaporation effects, when shallow lakes are compared to the larger and deeper ones, and thereby define a LEL (lake evaporation line) with a smaller slope than the other water types (Table 3). Seasonal and altitude effects cannot be evaluated owing to the small number of samples.

6) Both salinity and isotopic composition of fjord water in Ikka fjord illustrates well-defined vertical and horizontal mixing between fresh water from streams and precipitation and sea water entering from Davis Strait. The mixing between end members is highly correlated with R^2-values for the ^{2}H/^{18}O system of 0.99 and for the ^{18}O/salinity system of 0.98. The latter relation identifies different end member compositions from year-to-year both for inflowing sea water and fresh water. Seawater variations are caused by varying mixing in the Davis Strait between Polar Water from the East Greenland Current and North Atlantic Water from the Irminger Current, whereas freshwater variations reflect the seasonal shifts in precipitation.

7) Column water samples taken under water were contaminated to varying degrees by fjord water at the sampling sites. Least contamination was obtained by the syringe method, where water was extracted from the columns by aid of a syringe pump. Extrapolation to a chloride-free composition defines an uncontaminated column water composition of δ^2H = –102‰ and δ^{18}O = –14.2‰. This composition is identical to stream water sourced from winter precipitation at 500 m elevation at the carbonatite plateau and thus support the hypothesis that the Ikka columns are depending on a constrained ground water flow down through the igneous complex (Pauly 1963a; Buchardt *et al.* 1997; Buchardt *et al.* 2001).

8) Non-seasonal temporal effects in temperature and isotopic compositions are not clearly defined, and further studies are needed to evaluate the conflicting data reported by Seaman *et al.* (2022) and Stockmann *et al.* (2022).

Acknowledgements

References

Aðalsteinsdóttir, S.M. 2021: The low-temperature weathering of the Grønnedal-Íka Carbonatite Alkaline Silicate Igneous Complex in Southwest Greenland. Master's thesis, Faculty of Earth Sciences, University of Iceland, 82 pp.

Allaart, J.H. 1976: Ketilidian mobile belt in South Greenland. In: Escher, A. & Watt, W.S. (eds): Geology of Greenland, 120–151. Copenhagen: Geological Survey of Greenland.

Azetsu-Scott, K. & Tan, C. 1997: Oxygen isotope studies from Iceland to an East Greenland Fjord: Behavior of glacial meltwater plume. Marine Chemistry 56, 239–251. https://doi.org/10.1016/S0304-4203(96)00078-3

Bartels, A., Nielsen, T.F., Lee, S.R. & Upton, B.G. 2015: Petrological and geochemical characteristics of Mesoproterozoic dyke swarms in the Gardar Province, South Greenland: evidence for a major sub-continental lithospheric mantle component in the generation of the magmas. Mineral Magazine 79, 909–940. https://doi.org/10.1180/minmag.2015.079.4.04

Bauch, D., Hölemann, J., Andersen, N., Dobrotina, E., Nikulina, A. & Heidemarie Kassens, H. 2010: The Arctic shelf regions as a source of freshwater and brine-enriched waters as revealed from stable oxygen isotopes. Polarforschung 80, 127–140.

Bischoff, J.L., Fitzpatrick, J.A. & Rosenbauer, R.J. 1993: The solubility and stabilization of ikaite ($CaCO_3 \cdot 6H_2O$) from 0°C to 25°C: environmental and paleoclimatic implications for thinolite tufa. Journal of Geology 101, 21–33. https://doi.org/10.1086/648194

Bondam, J. 1992: The Grønnedal-Ika alkaline complex in South Greenland: review of geoscientific data relevant to explora-tion. Open File Serie, Grønlands Geologiske Undersøgelse 92/2, 28 pp.

Bonne, J.-L., Masson-Delmotte, V., Cattani, O., Delmotte, M., Risi, C., H. Sodemann, H. & Steen-Larsen, H.C. 2014: The isotopic composition of water vapor and precipitation in Ivittuut, southern Greenland. Atmospheric Chemistry and Physics 14, 4419–4439. https://doi.org/10.5194/acp-14-4419-2014

Buch, E. 1995: Havstrømme omkring Grønland. In: Gregersen, S. (ed.): Grønlands fysiske natur, 25–32. Copenhagen: Rhodos.

Buch, E. 2002: Present oceanographic conditions in Greenland Waters. Danish Meteorological Institute Scientific Reports 2002-02, 39 pp.

Buchardt, B., Seaman, P., Stockmann, G., Vous, M., Wilken, U., Düwel, L., Kristiansen, A., Jenner, C., Whiticar, M.J. & Kristensen, R.M. 1997: Submarine columns of ikaite tufa. Nature 390, 129–130. https://doi.org/10.1038/36474

Buchardt, B., Israelson, C., Seaman, P. & Stockmann, G. 2001: Ikaite tufa towers in Ikka Fjord, Southwest Greenland: their formation by mixing of seawater and alkaline spring water. Journal of Sedimentary Research 71, 176–189. https://doi.org/10.1306/042800710176

Callisen, K., 1943: Igneous rocks of the Ivigtut region, Greenland; Part 1, the nepheline syenites of the Grønnedal-Ika area. Meddelelser om Grønland 131(8), 74 pp.

Clark, I. D. & Fritz, P. 1997: Environmental isotopes in hydrogeology, 328 pp. New York: Lewis Publishers.

Craig, H. 1961: Isotopic variations in meteoric waters. Science 133, 1702–1703. https://doi.org/10.1126/science.133.3465.1702

Dahl, K. & Buchardt, B. 2006: Monohydrocalcite in the Arctic Ikka fjord, SW Greenland: first reported marine occurrence. Journal of Sedimentary Research 76, 460–471. https://doi.org/10.2110/jsr.2006.035

Dansgaard, W. 1964: Stable isotopes in precipitation. Tellus 16, 436-468. https://doi.org/10.1111/j.2153-3490.1964.tb00181.x

Darling, W.G. & Talbot, J. C. 2003: The O and H stable isotope composition of freshwaters in the British Isles. 1. Rainfall. Hydrology and Earth System Sciences 7, 163–181. https://doi.org/10.5194/hess-7-163-2003

Darling, W., Bath, G.A.H. & Talbot, J.C. 2003: The O and H stable isotope composition of freshwaters in the British Isles. 2. Surface waters and groundwater. Hydrology and Earth System Sciences 7, 183–195. https://doi.org/10.5194/hess-7-183-2003

Emeleus, C.H. 1964: The Grønnedal-Ika alkaline complex, South Greenland. The structure and geological history of the complex. Bulletin Grønlands Geologiske Undersøgelse 45, 75 pp. https://doi.org/10.34194/bullggu.v45.6579

Fristrup, B. 1971: Grønland. Klimatologi og glaciologi. In: Nørrevang, A., Meyer, T.J. & Christensen, S. (eds): Danmarks Natur, 136–176. Copenhagen, Politikens Forlag.

Hansen, M. O., Buchardt, B., Kühl, M., & Elberling, B. 2011: The fate of submarine ikaite tufa columns in southwest Greenland under changing climate conditions. Journal of Sedimentary Research 81, 553–561. https://doi.org/10.2110/jsr.2011.50

Granskog, M. A., Kuzyk, Z. Z. A., Azetsu-Scott, K., & Macdonald, R. W. 2011: Distributions of runoff, sea-ice melt and brine using $\delta^{18}O$ and salinity data – A new view on freshwater cycling in Hudson Bay. Journal of Marine Systems 88, 362–374. https://doi.org/10.1016/j.jmarsys.2011.03.011

International Atomic Energy Agency 1969: Environmental isotope data No. 1: World survey of isotope concentration in precipitation (1953-1963). Technical Reports Series No. 96, 422 pp. Vienna.

International Atomic Energy Agency 1970: Isotope data No. 2: World survey of isotope concentration in precipitation (1964-1965). Technical Reports Series 117, 402 pp. Vienna.

International Atomic Energy Agency 1971: Environmental isotope data No. 3: World survey of isotope concentration in precipitation (1966-1967). Technical Reports Series 29, 402 pp. Vienna.

International Atomic Energy Agency 1973: Environmental isotope data No. 4: World survey of isotope concentration in precipitation (1968-1969). Technical Reports Series 147, 334 pp. Vienna.

International Atomic Energy Agency 1975: Environmental isotope data No. 5: World survey of isotope concentration in precipitation (1970-1971). Technical Reports Series 165, 309 pp. Vienna.

International Atomic Energy Agency 1979: Environmental isotope data No. 6: World survey of isotope concentration in precipitation (1972-1975). Technical Reports Series 192, 187 pp. Vienna.

Kristiansen, J. & Kristiansen, A. 1999: A new species of *Chroomonas* (Cryptophyceae) living inside the submarine ikaite columns in the Ikkafjord, southwest Greenland, with remarks on its ultrastructure and ecology. Nordic Journal of Botany 19, 747–758. https://doi.org/10.1111/j.1756-1051.1999.tb00684.x

Leng, M.J. & Adderson, N.J. 2003: Isotopic variations in modern lake waters from western Greenland. The Holocene 13, 605–611. https://doi.org/10.1191/0959683603hl620rr

Östlund, H.G. & Hut, G. 1984: Arctic Ocean water mass balance from isotope data. Journal of Geophysical Research: Oceans 89(C4), 6373–6381. https://doi.org/10.1029/JC089iC04p06373

Pauly, H. 1963a: Ikait, nyt mineral der danner skær. Naturens Verden 168–192.

Pauly, H. 1963b: "Ikaite", a new mineral from Greenland. Arctic 16, 263–264. https://doi.org/10.14430/arctic3545

Priem, A. & Stougaard, P. 2006: Bacterial diversity in permanently cold and alkaline ikaite columns from Greenland. Extremophiles 10, 551–562. https://doi.org/10.1007/s00792-006-0529-9

Ranta, E., Stockmann, G., Wagner, T., Fusswinkel, T., Sturkell, E., Tollefsen, E. & Skelton, A. 2018: Fluid-Rock reactions in the 1.3 Ga siderite carbonatite of the Grønnedal-Íka alkaline complex, Southwest Greenland. Contributions to Mineralogy and Petrology 173, 1–28. https://doi.org/10.1007/s00410-018-1505-y

Rogers, J.J. & Santosh, M.J.G.R. 2002: Configuration of Columbia, a Mesoproterozoic supercontinent. Gondwana Research 5, 5–22. https://doi.org/10.1016/S1342-937X(05)70883-2

Rozanski, K., Araguás-Araguás, L. & Gonfiantini, R. 1993: Isotopic patterns in modern global precipitation. Climate change in continental isotopic Records 78, 1–36. https://doi.org/10.1029/GM078p0001

Schmidt, M., Priemé, A. & Stougaard, P. 2006: Bacterial diversity in permanently cold and alkaline ikaite columns from Greenland. Extremophiles 10, 551–562. https://doi.org/10.1007/s00792-006-0529-9

Seaman, P.G. 1998: The development of Ikaite in a Fjord environment with special reference to Ikka Fjord. Unpublished. Ph.D. Thesis, Imperial College of Science, Technology and Medicine, University of London, London, UK, 263 pp.

Seaman, P. & Buchardt, B. 2006: The columns of ikaite tufa in Ikka Fjord, Greenland. Meddelelser om Grønland Geoscience 44, 39 pp. https://doi.org/10.7146/moggeosci.v44i.140293

Seaman, P., Sturkell, E., Gyllencreutz, R., Stockmann, G.J. & Geirsson, H. 2022: New multibeam mapping of the unique *Ikaite* columns in Ikka Fjord, SW Greenland. Marine Geology 222, 1–14. https://doi.org/10.1016/j.margeo.2021.106710

Stockmann, G. & Wilken, U. 2007: Ikkasøjlerne – en undersøisk oase i Arktis, 85 pp. Copenhagen: Dansk Polarcenter.

Stockmann G., Karlsson, A., Lewerentz, A., Thomsen, T.B., Kokfelt, T.F., Tollefsen, E., Sturkell, E. & Lundqvist, L. 2018a: New Rb–Sr and zircon U–Pb dating of the Grønnedal-Íka igneous complex, SW Greenland. Nordic geological winter meeting 2018, Copenhagen, Denmark. Abstract volume, p. 38.

Stockmann, G., Tollefsen, E., Skelton, A., Brüchert, V., Balic-Zunic, T., Langhof, J., Skogby, H. & Karlsson, A. 2018b: Control of calcite inhibitor (phosphate) and temperature on ikaite precipitation in Ikka fjord, southwest Greenland. Applied Geochemistry 89, 11–22. https://doi.org/10.1016/j.apgeochem.2017.11.005

Stockmann, G.J., Seaman, P., Balic-Zunic, T., Peternell, M., Sturkell, E., Liljebladh, B. & Gyllencreutz, R. 2022: Mineral changes to the tufa columns of Ikka Fjord, SW Greenland. Minerals 12, 1430. https://doi.org/10.3390/min12111430

Stougaard, P., Jorgensen, F., Johnsen, M.G. & Hansen, O.C. 2002: Microbial diversity in ikaite tufa columns: An alkaline, cold ecological niche in Greenland. Environmental Microbiology 4, 487–493. https://doi.org/10.1046/j.1462-2920.2002.00327.x

Sørensen, M.V. & Kristensen, R.M. 2000: Marine rotifera from Ikka fjord, SW Greenland. Meddelelser om Grønland, Bioscience 51, 46 pp. https://doi.org/10.7146/mogbiosci.v51.142614

Tappa, D. J., Kohn, M. J., McNamara, J. P., Benner, S. G. & Flores, A. N. 2016: Isotopic composition of precipitation in a topographically steep, seasonally snow-dominated watershed and implications of variations from the global meteoric water line. Hydrological Processes 30, 4582–4592. https://doi.org/10.1002/hyp.10940

Thorbjørn L. & Petersen G.H. 2003: The epifauna on the carbonate reefs in the Arctic Ikka Fjord, SW Greenland. Ophelia 57, 177–202. https://doi.org/10.1080/00785236.2003.10409513

Tollefsen, E., Stockmann, G., Skelton, A., Mörth, C.-M, Dupraz,

C. & Sturkell, E. 2018: Chemical controls on ikaite formation. Mineralogical Magazine 82, 1119–1129. https://doi.org/10.1180/mgm.2018.110

Tollefsen, E., Stockmann, G., Skelton, A., Lundqvist, L. & Sturkell, E. 2019: Secondary alteration of the Grønnedal-Ika igneous complex and the genesis of ikaite, $CaCO_3$ $6H_2O$, SW Greenland. Chemical Geology 510, 18–30. https://doi.org/10.1016/j.chemgeo.2019.02.009

Trampe, E.C., Larsen, J.E., Glaring, M.A., Stougaard, P. & Kühl, M. 2016: In situ dynamics of O_2, pH, light, and photosynthesis in ikaite tufa columns (Ikka fjord, Greenland) – a unique microbial habitat. Frontiers of Microbiology 7, 722. https://doi.org/10.3389/fmicb.2016.00722

Trampe, E. C., Castenholz, R.W., Larsen, J.E. & Kühl, M. 2017: Phototrophic microbes form endolithic biofilms in ikaite tufa columns (SW Greenland). Environmental Microbiology 19, 4754–4770. https://doi.org/10.1111/1462-2920.13940

Upton, B.G.J. 2013: Tectono-magmatic evolution of the younger Gardar southern rift, South Greenland. Geological Survey of Denmark and Greenland Bulletin 29, 128 pp. https://doi.org/10.34194/geusb.v29.4692

Vester, J. K., Lylloff, J. E., Glaring, M. A. & Stougaard, P. 2013: Microbial diversity and enzymes in ikaite columns: a cold and alkaline environment in Greenland. Polyextremophiles: Life Under Multiple Forms of Stress, 365–380. https://doi.org/10.1007/978-94-007-6488-0_15

Weidick, A., Kelly, M. & Bennike, O. 2004: Late Quaternary development of the southern sector of the Greenland Ice Sheet, with particular reference to the Qassimiut lobe. Boreas 33, 284–299. https://doi.org/10.1111/j.1502-3885.2004.tb01242.x